Embedded Sensors for Next Generation Composite Materials

By:

José Miguel Barragán Martinez

Thesis submitted to the University of Ottawa in partial fulfilment of the requirements for the program of Master of Applied Science Chemical Engineering.

Department of Chemical and Biological Engineering

Faculty of Engineering

University of Ottawa

MASc in Chemical Engineering (2026)

FACULTY: Faculty of Engineering

DEPARTMENT: Chemical and Biological Engineering

INSTITUTION: University of Ottawa

TITLE: Embedded sensors for next generation composite materials

AUTHOR: José Miguel Barragán, BASc, CPO.

SUPERVISORS: Dr. Chantal Paquet, Ph.D.; Dr. Benoît H Lessard, P.Eng., M.Eng., Ph. D.

PAGES : 95

A. Abstract

This master's thesis presents the development and optimization of next generation embeddable sensors for aerospace composite monitoring. All work was done in collaboration with the NRC's Quantum and Nanotechnology Research Centre, NRC's Aerospace Research Centre, and the University of Ottawa's Lessard Research Group.

This thesis is divided into 4 chapters; a literature review, which highlights the importance of this research, the key aspects of embedded sensing, and compares existing embedded measuring technologies for composite materials, drawing attention to the fact that all existing technologies present drawbacks in the form of elevated costs, high complexity, low resilience, extreme sensitivity to factors such as temperature and pressure, and most critically, degrading the structural integrity of the composite material in which they're embedded.

The second chapter shows a proof of concept for next generation sensors, which would have small enough footprint to not affect the composite performance, as well as be resilient enough to survive throughout the entire service life of the component, regardless of conditions faced. These sensors proved to be effective in measuring a common manufacturing defect known as ply migration, with an accuracy of 0.6mm.

The third chapter proposes the second generation of the embedded sensors, which aimed to improve their performance to the point of being able to measure strain and damage to the composite, whilst retaining all the abilities from the previous generation. This was achieved through an improved shape and sensor architecture, with the ability to measure return signal loss when the composite was under stress, and a permanent loss when the composite suffered damage to its matrix. Lastly, the conclusion provides an insight into future work to be done and recaps the advancements achieved throughout the course of the research.

B. Acknowledgments

First and foremost, I would like to thank Dr. Chantal Paquet from the NRC Quantum and Nanotechnology Research Centre. She has been an outstanding mentor, advisor, and believer in this research and myself. Only thanks to her time, energy, and patience is this work possible.

I would also like to thank the extraordinary team at the NRC Aerospace Research Centre. Catalin, Drazen, and Marc never hesitated to provide effort and vast technical knowledge without which any advancement in this project would have taken lifetimes. They truly helped shape and elevate the work presented into cutting edge research, even breaking the cardinal rule of not running experiments on Friday to help me complete this thesis.

Of course, none of this would have been possible without Professor Benoît Lessard's invitation to join his research group, and subsequent projects with the NRC. To him I owe the incredible opportunity of being allowed to follow my passion for aerospace-themed chemical engineering research.

I also cannot thank my dad, mom, and grandad enough for their support throughout my bachelor's and master's degrees. Despite facing unprecedented times, and being a considerable distance away, their support and guidance has allowed me to focus on my work and truly enjoy it.

Lastly, I would like to thank you, the reader, who by going through the pages presented in this thesis makes it all worth it. Being able to share this exciting work with others is truly a reward on its own.

C. Table of Contents

D. List of Figures

Key Abbreviations

CFRP: Carbon fiber reinforced polymer

EC: Eddy currents

FBG: Fibre Bragg Grating

Prepreg: Preimpregnated carbon fiber laminate

RF: Radio frequency

ITD: Incipient thermal damage

LIG: Laser induced graphene

IR: Infra-red

NRC: National Research Council Canada

UAV: Unmanned aerial vehicle

NDT: Non-destructive testing

SSNP: Single-sided non-plated coil sensor

DSNP: Double-sided non-plated coil sensor

SSCP: Single-sided plated coil sensor

DSCP: Double-sided plated coil sensor

KT: Polyimide encapsulated disc sensor printed on 1 mil polyimide, 1-3 layers

TT: Disc sensor directly in contact with the composite, printed on 1 mil polyimide, 1-3 layers.

TR: Disc sensor directly in contact with composite, printed on 5 mil polyimide, 1-3 layers.

KR: Polyimide encapsulated disc sensor printed on 5 mil polyimide, 1-3 layers.

1. Introduction

1.1 Background

1.1.1 Composite Materials: CFRP

Carbon fiber reinforced polymers (CFRP) are widely used as structural materials in aerospace, automotive, and naval sectors, to reduce vehicle weight and fuel consumption. This is mainly due to their superior specific strength and stiffness properties[1], especially when compared to steel and aluminum, other common manufacturing materials in these industries.

CFRP parts can be manufactured with a large variety of techniques, but this thesis will focus solely on parts made by sequentially laying up carbon fiber fabrics pre-impregnated in a thermosetting matrix (prepregs). Prepregs, as their name indicates, come pre-impregnated with a strictly controlled amount of epoxy or thermoset resin that is injected when initially manufactured. These types of composites offer superior consistency and performance for aerospace-grade applications[2]. Pre-impregnated composites are the most prevalent for aerospace primary structures due to their high fiber volume fraction, low void content, and precise resin control, which are difficult to achieve with liquid molding techniques.[1] Prepregs require cold storage and autoclave curing under high temperature and pressure, as well as strictly following curing protocols specified by the manufacturer, to fully consolidate the laminate and achieve optimal mechanical properties. Unidirectional fibers are used for primary load-bearing elements due to their high directional stiffness. Aerospace-grade resins include high-performance epoxies with elevated glass transition temperatures ($T_g > 180°C$), often toughened with thermoplastic particles to enhance impact resistance and delamination behavior[3]. While prepregs offer excellent material quality and are ideal for embedding sensors or achieving clean laminate interfaces, they come with significant drawbacks: high cost, limited shelf life, and the need for precise processing

environments. Despite this, their performance and reliability make them the material of choice for aircraft skins, spars, fuselages, and other flight-critical structures.

However, unlike metal forming processes which involve plastic deformation of homogeneous materials, composite forming relies on inducing targeted inter- and inner- ply-slip.[5] Having the ability to constantly, and non-destructively, verify the state of health of a composite can enhance safety and efficiency in a variety of industries where they are mission-critical.

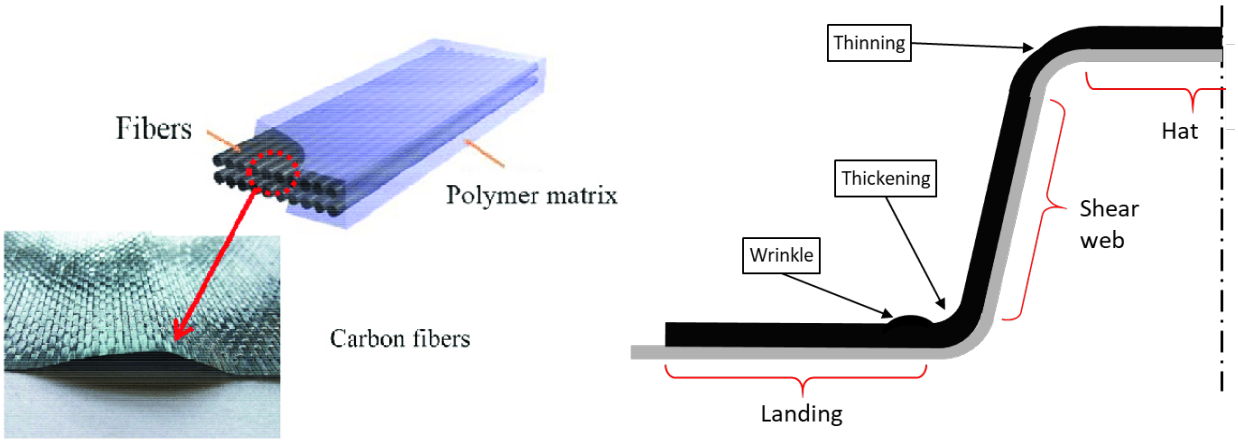

***Figure 1**: Diagram of a CFRP, showing the interaction between the fibers and the matrix (L), diagram showing possible defects of a CFRP when manufacturing (R).*

1.1.2 Importance of Composite Material Measurement

Manufacturing CFRP is a sensitive process, and if not conducted properly, it can cause a range of adverse effects, such as corner thickening / thinning or ply wrinkling, which compromises the structural integrity of the part.[4–7] Post-manufacturing, the composite material will also endure thermal and mechanical stresses throughout its life cycle.[8] Furthermore, exceeding the design parameters of a composite (thermal, mechanical) results in catastrophic failure.[2] There's a push for development of continuous or discrete measurement of properties for next generation composite materials, in order to better understand the material evolution throughout its useful life.

1.2 Measurement of Composite Materials

1.2.1 Measurable Properties

There's a wide variety of properties that can be measured continuously or discretely, for the purposes of this thesis, we'll focus only on non-destructive measuring of health and strain. Strain is a key parameter to measure because of catastrophic failure when too much force is put into a composite. Strain sensors measure how much stress a composite has been put under. This parameter measurement is ideally continuous to immediately known whether safe operational parameters have been exceeded.[9] Health and damage will be used as an interchangeable term in this thesis, they represent the degradation of the polymer composite matrix, which occurs as the CFRP goes through its life cycle and experiences mechanical and thermal stresses.[10] Other key parameters, such as temperature, ply migration during manufacturing, and remaining useful life of a composite fall beyond the scope of this thesis but remain interesting fields of research.[11].

1.2.2 Key Considerations

Different materials and technologies can be used for the manufacturing sensors, these directly depend on the application for which the sensor will be used. The first aspect to consider is cost effectiveness of the sensor. Some sensors can be of very low cost to develop and implement, they focus on reducing the cost of the process/raw materials such as those which rely only on slight modifications to the CFRP itself to measure damage. These are ideal for large scale implementation or single use pieces.[12,13] Another important aspect is the temperature range the sensor will operate under. Aerospace applications require sensors to endure temperatures of over 200°C and under -40°C to be approved for commercial application. To achieve functionality over this wide range of temperature, different materials such as fiber optics, silver molecular ink, and even thermochromic paint have been used.[14–16] Size factor is another critical aspect to consider,

sensors can go from being as thin as a few microns ($< 25\mu m$) up to a couple millimeters ($> 5000\mu m$). Embedding is another key aspect to consider, once a sensor is embedded, it becomes a part of the CFRP piece, which provides protection from the elements and allows for easier large-scale implementation. However, embedding limits the thickness of the sensor to half of that of a CFRP ply (one ply is around 135 um), and maximum area of 1.6 cm2, it also means that the sensor should be ideally wireless or it's prone to cause manufacturing defects.[1,2] Not embedding allows for larger sensors, makes them easily replaceable, but also more prone to damage and more difficult to implement.[17,18] Robustness or resilience of a sensor is also important to keep in mind. Not all sensors and materials are built the same, this is particularly noticeable in the useful life of each. Whereas some of them are embeddable and are only limited by the useful life of the composite, such as RF/EC damage sensors, some others like piezoresistive strain sensors are only useful for 100 cycles.[19–21] Aircraft skin which is subject to lots of flexing but is only affected by damage would be an ideal use for the former, whereas structural spars which shouldn't flex would be better suited for the latter.[2] Precision and sensitivity of a sensor is another key parameter to measure. Damage detection can be measured with deviations as little as 3mm from the damaged area and sensors indicate damage as soon as the matrix starts breaking down or has been operated beyond ideal parameters.[19,22,23] Strain detection is affected by the gauge factor (sensitivity) of the sensor and needs to be carefully tuned for the material.[24].

1.2.3 Limitations of Current Technologies

For every benefit a specific material and technology brings, there are also some limitations which must not be overlooked. The largest limitation for most sensors is temperature, especially for strain sensors. Most strain sensors are incredibly sensitive to temperature changes. Changes as low as 10°C can have an impact of over 15% in the readout values, however these can be fixed

with better algorithms to interpret the data.[26] Another limitation is the resistance of technologies to impact damage. Impacts are known to disrupt the equipment for most of the fiber optics-based sensors, either the fiber optic cable itself will break or the necessary equipment to make it work will.[27–29] Lastly, the complexity of the system can substantially limit where the sensor can be placed. Generally, the accuracy of the sensor is directly proportional to its complexity. The best example of this is the fiber optic-based sensors, which offer super accuracy but require lots of hardware to function, including laser emitters, receivers, a computer to interpret the data and advanced signal processing algorithms to translate it correctly.[30] Other embedded sensors like acoustic and RF ones require lots of additional equipment and do not offer continuous measurements.[31] Overall, there is not a sensor that could be defined as the best, but every sensor and technology has its niche application where its benefits outweigh the drawbacks, or where the limitations are avoided altogether. Below, a literature review of different technologies used for sensing strain and damage in composites.

1.3 Sensing Technologies

1.3.1 Microgrids

Microgrids consist of adding conductive filaments to the CFRP weave, and then measuring changes in electrical signal to assess damage. They are advantageous because they offer high precision damage detection as a directly embeddable solution. They're sensitive and accurate but presents serious structural integrity drawbacks for the CFRP, which reduces its attractiveness for large scale application.[31] Current microgrids are mainly based on copper strands, which yield highly accurate results with detection as good as 10mm away from the damage site.[19] The main problem with this material is that embedding metal in the CFRP reduces its performance significantly. This is because copper can oxidize and damage the composite from the inside, greatly

reducing its structural integrity and the useful life of the composite.[32] Overall, microgrids offer good damage detection and are easily embeddable, though they're limited by a reduction in structural integrity for metallic based sensors.

1.3.2 Optical Fiber Sensors

These systems use embedded fiber optic cables in the carbon weave or between the layers of carbon fiber. It offers great precision for both strain and damage sensing but is also the most difficult and technically complex sensor to develop. There are two main architectures for fiber optic sensors, the first is Fabry-Perot interferometric sensors, which work by measuring the interference of multiple beams of light. They offer larger ranges of strain (up to 135%) than Bragg Grating sensors. They require complex computational analysis of the data to interpret it correctly and are affected by temperature changes as low as 10°C. They are also thicker than the Bragg Grating counterparts at 300um, which is thick enough to disrupt the structural integrity of the composite material.[25–27] The other architecture used is Fiber Bragg Grating, which works by measuring the diffraction of a single beam of light. It has a much thinner fiber optic cable (125 um) but also slightly lower strain capabilities (only up to 120%). However, it shares all the limitations Fabry Perot sensors do, such as complex software, extensive hardware, and sensitivity to temperature changes and impact.[29] Different materials have also been explored for the fiber optics, a study in 2018 combined the Bragg Grating fiber optic technology, but instead of using a glass fiber it used a polymer specifically developed for this application. This greatly reduces cost and susceptibility to impact in the fiber itself, and makes the sensor a lot more flexible, allowing up to 1.4% elongation which is impossible for glass-based fibers.[30] Another proposition is to combine the hardware from the Bragg Grating technology (thinner, better performing fibers), with the measuring mechanisms and software of Fabry Perot sensors. This, in addition to newly

developed algorithms for data interpretation, reduces the impact of changing temperatures in the precision of the measurement up to 80°C.[25] Optical fiber-based technologies are the best performing for extremely accurate measurements, and can maintain this performance for a virtually unlimited number of cycles.

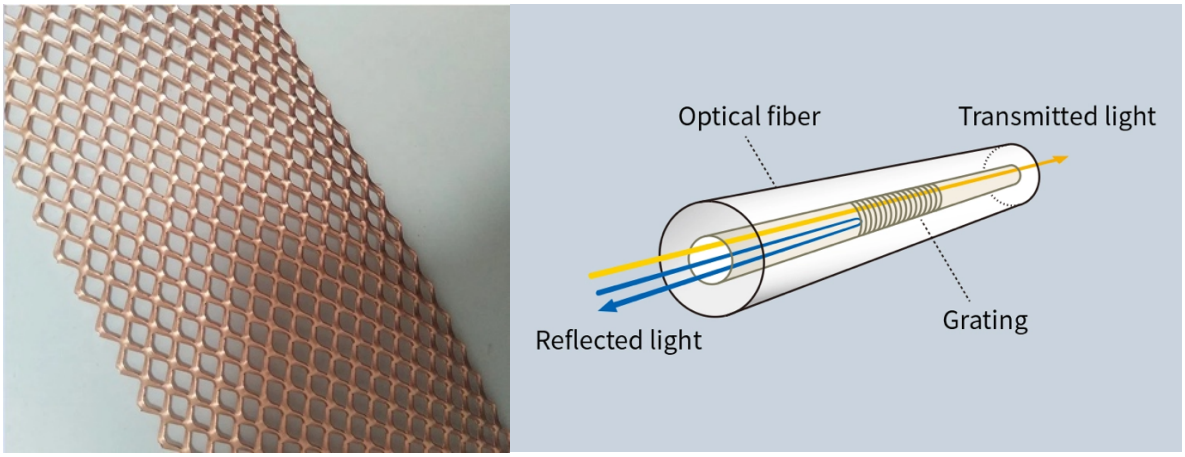

Figure 2: *Copper microgrids for damage measurement (L), Bragg Grating Fiber diagram (R)*

1.3.3 Piezoresistive Materials

Laser-Induced Graphene (LIG) was proposed by Carvalho et al.[33] as an approach for embedded strain sensing, particularly because it transforms the surface of a polyimide, like kapton, into a porous, conductive graphene network using laser irradiation. While most existing LIG processes rely on infrared (IR) lasers, Carvalho's work presents a UV-laser-based method that produces comparable graphene structures but with improved spatial resolution and shallower penetration depth (~5 μm). This makes it especially useful for thin-film or layered applications where material intrusion must be minimal. The resulting graphene network functions as a piezoresistive material, meaning its electrical resistance changes in response to mechanical deformation. This behavior allows it to act as a passive strain sensor without the need for external transduction mechanisms. Unlike many piezoresistive composites that rely on dispersed carbon black or CNTs within a polymer matrix, LIG forms a monolithic, intrinsically conductive film

directly on the substrate, reducing variability and improving signal clarity. The UV-LIG sensors demonstrated in the study show a gauge factor up to 20, low hysteresis, and consistent linear response to strain, pressure, and bending. The performance is tunable by adjusting the thickness of the underlying polyimide films. Thinner films (like Kapton HN200) are more sensitive to micro-scale forces and useful for wearable biosensing (e.g., pulse monitoring), while thicker substrates (like HN500) expand the strain range and improve mechanical robustness, making them more suitable for structural health monitoring and soft robotics. However, this technology has the limitation of being very expensive to develop, fragile, and if embedded into composites, it would require a considerable reduction in mechanical performance and integrity, due to the fact it needs leads to work, and the inclusion of a material that's not compatible with the epoxy matrix.

1.3.4 Thermochromic sensing

Thermochromic polymer film sensors offer a passive, non-invasive method for detecting incipient thermal damage (ITD) in carbon fiber-reinforced epoxy composites. Unlike physical defects such as delamination or cracks, ITD begins with chemical degradation changes in matrix chemistry that can significantly reduce mechanical properties long before conventional methods like ultrasonic C-scans detect any damage. Toivola et al.[16] developed a smart polymer film incorporating a specially designed molecule (M1) that transitions irreversibly from a non-fluorescent to a fluorescent state upon exposure to critical thermal conditions. This change is triggered by a retro-Diels–Alder reaction and corresponds closely with the time-temperature thresholds associated with the onset of ITD. The molecule is embedded in a PDMS matrix, forming a flexible sensor film that is applied to the composite surface and removed post-exposure. These sensors visually indicate whether damaging thermal events have occurred, using UV-induced fluorescence as the readout. Compared to other techniques, the key advantage lies in the film's

ability to accumulate thermal history capturing not just the peak temperature, but also the duration of exposure. This enables accurate detection of thermal degradation that standard ultrasonic C-scans or mechanical tests might miss. The films demonstrated sensitivity to damage exposure as low as 180 °C for 10 minutes, with clear fluorescence correlating to reductions in interlaminar shear strength (ILSS). Furthermore, they can be easily integrated over wide areas using adhesives, without wiring or embedded electronics. However, their main limitations include single-use operation, dependence on UV/optical readout tools for quantification, and the need for consistent surface contact. Lastly, they may interfere or damage with already existing coatings that may be on the composite material, such as radar absorbing materials, which limits their applications.

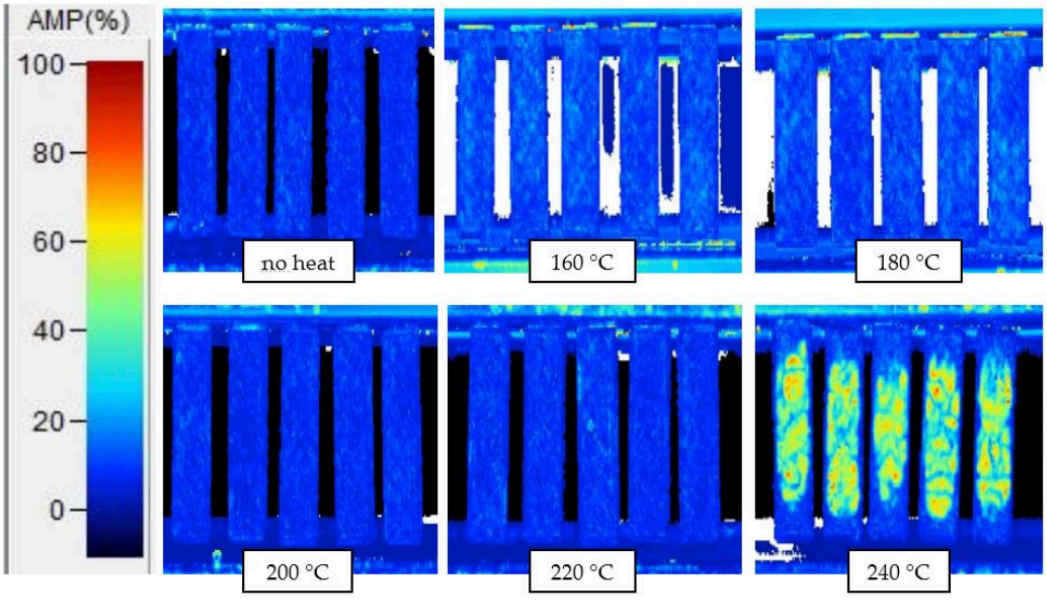

***Figure 3**: C-scans showing amplitude of interior reflections from short-beam samples exposed to various temperatures for 1 h.*

1.3.5 Acoustic Sensing

Optical fibre acoustic emission sensors are another approach for embedded sensing within a composite, particularly for real-time damage detection. This approach was proposed in different papers by Read et al. and Huijer et al. [34,35]. These sensors offer the advantage of being compact, lightweight, and capable of detecting high-frequency acoustic emissions generated during damage events such as delamination, fibre breakage, or matrix cracking. The sensing mechanism is based on a Fabry–Perot interferometric cavity formed between two fibre end faces inside a capillary tube, which allows strain waves to modulate the intensity of reflected light. This modulation can be used to detect acoustic events with high sensitivity, even in large-scale aerospace components. Trials have shown that both surface-mounted and embedded configurations can detect emission events, with recorded signal frequencies typically around 150 kHz well above the ambient noise threshold. However, several limitations remain. The sensors are highly sensitive to strain and temperature, which means that maintaining signal stability requires either continuous wavelength tracking or dual-laser demodulation systems, increasing system complexity. Additionally, the signal-to-noise ratio is still a limiting factor, particularly for low-energy damage events, and the current signal processing was done offline, highlighting the need for more integrated, real-time systems. Lastly, by the time of writing, there was little acoustic damage data on composites to compare with, which might become less of a problem as the technology matures.

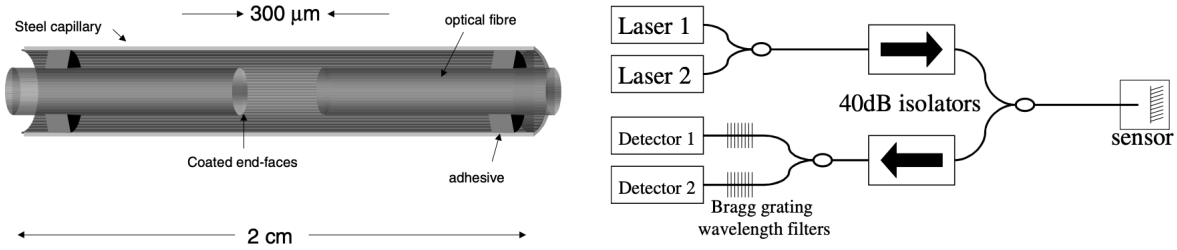

***Figure 4**: Optical Fiber acoustics emissions sensor (left), optical sensing system (right).*

1.3.6 Microwave Sensing

Microwave sensors operate by transmitting high-frequency electromagnetic waves into the composite and analyzing the reflected signal to detect internal damage or material changes. In CFRP structures, microwave-based sensing is especially attractive because it allows for non-contact, one-sided inspection with relatively simple hardware, making it suitable for both surface scanning and embedded monitoring applications. These sensors are advantageous due to their ability to penetrate dielectric layers and detect defects such as delamination, fiber breakage, voids, and moisture ingress[22,36]. Compared to fiber-optic-based methods, microwave sensors are not affected by surface coupling or the need for immersion, which makes them faster and more adaptable to in-field use. Modern systems can detect defects as small as 0.2 mm, particularly when using open-ended waveguide probes or microstrip antenna arrays. However, a major limitation of microwave sensors is their limited penetration depth, especially in high-conductivity or thick composite sections. To achieve a spatial resolution 5mm, the frequency must be increased up to 24 GHz. However, at that frequency the penetration is less than 1mm into the CFRP, much less than the industry standard maximum depth of 4mm for structural composite pieces[36]. To compensate for this, frequency must be reduced to 10 GHz or less, reducing the resolution to 20mm. This limits their effectiveness for deep or multilayered damage detection. Additionally, the anisotropic and lossy nature of CFRP can distort signal behavior, requiring advanced calibration and interpretation models.

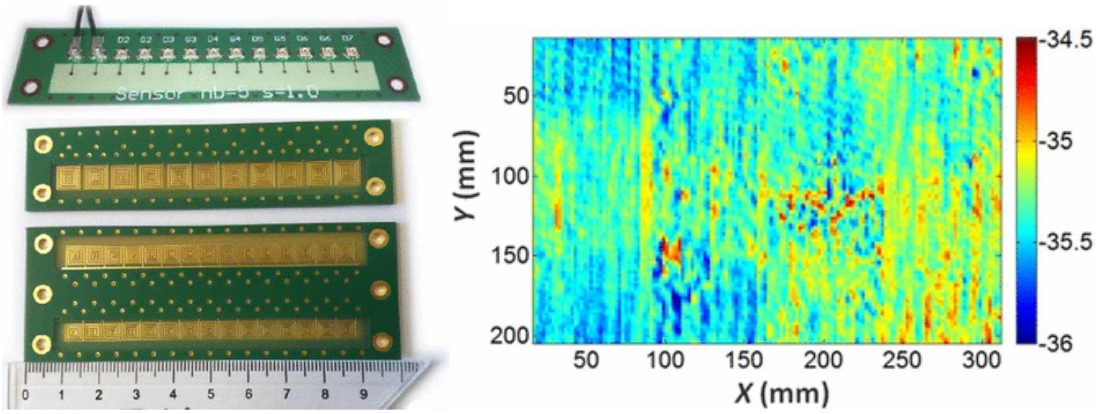

***Figure 5**: Microwave sensor (left) and scan (right) of a composite piece.*

1.3.7 Eddy Currents

Another approach for delamination detection in CFRP uses eddy currents to focus on power loss rather than traditional induced voltage signals. This approach was developed by Wang et al.[37] CFRP's low through-thickness conductivity makes conventional eddy current testing ineffective for internal damage, since the signal is often too weak and easily overwhelmed by noise. To get around this, a vertical 8-shaped coil was developed that generates a concentrated vertical eddy current field, specifically targeting interlaminar defects. When delamination occurs, the eddy current loop is disrupted, which reduces the total energy dissipated in the material. This loss is measured directly using a parallel LC resonance circuit and a micro-power detection module, which replaces the traditional voltage-based signal acquisition. Because the signal is based on absolute power loss rather than differential voltage, it's more robust to environmental interference and background noise. The setup works best at low frequencies (around 750 kHz), which is ideal for embedded systems since it reduces both hardware complexity and power consumption. Compared to traditional ECT, it delivers better sensitivity to internal delamination even with lower-frequency excitation and smaller, simpler electronics. However, like most near-field sensing systems, lift-off is a limiting factor — performance begins to drop off beyond 3 mm,

and becomes unreliable past 7 mm. It also outperformed circular and square coil geometries, with up to a 19.6% change in signal across defect sites, confirming that vertical coil orientation is critical for through-thickness sensitivity. The method has also been validated on both artificially induced and real-world delaminations, showing potential for automated scanning and embedded structural health monitoring.

A new approach to eddy current sensors will be the focus of this thesis. As seen in the previous example, EC sensors usually rely on an embedded target actively sending out a signal, and a probe that measures the difference and inconsistencies in signal across the composite in order to find damages. The sensors presented in this thesis are passive, meaning that they do not require an active energy source physically connected to them, yet still provide meaningful readouts thanks to their difference in material (manufactured out of silver ink) compared to CFRP. They present the advantage that they can be very thinly manufactured, embedded without disrupting structural integrity, and measured wirelessly. They can measure temperature, strain, ply migration defects as well as damage to a composite. Their main limitations are that they cannot constantly monitor the output of the sensors, and that their sensitivity for damage and strain is still limited compared to more established technologies .[21] However, and unlike other technologies mentioned in this review, they are not costly to implement, are simple to manufacture, do not affect the structural integrity of this composite, are impervious to temperature changes, and can survive throughout the service life of the composite piece, providing useful data throughout. There has been success with this technology with ply migration defects down to 0.3mm precision[38], as well as strain and damage sensing, as will be presented in chapters 2 and 3 of this thesis respectively.

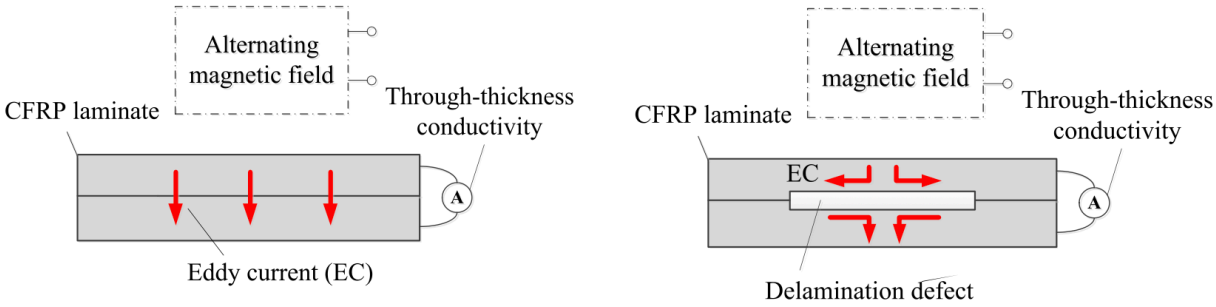

Figure 6: *Undamaged (left) and delaminated (right) composites, showing how the change would affect the measurement*

1.4 Research Objectives

Aware of existing limitations of non-destructive testing technologies for monitoring the state of an aerospace composite (CFRP) throughout its service life, I collaborated with the NRC Aerospace Research Centre, NRC Quantum and Nanotechnology Research Centre, and the Lessard Research Group, to design and manufacture the next generation of sensors. At the very beginning of the project, several stringent requirements based on industry standards were established in order to consider our sensors viable, as well as some KPI's that would be interesting to track in a composite via the embedded sensors; these included limitations in size (smaller than 161 mm2), thickness (thinner than half a ply of pre-impregnated composite, 0.0675 mm), survivability (200°C to -200°C, 0 to 6 bar) and performance (readable through at least 4mm of composite, the industry standard highest thickness for a part). They also suggested that the ability to monitor ply migration, manufacturing defects, damage, strain, and temperature, would be incredibly useful in such a package. We decided that next generation eddy current sensors, which would work as embeddable targets to measure manufacturing defects, matrix damage, and strain would answer those requirements.

In other words, the NRC had a well-established criterion based on aerospace industry standards for future composite health monitoring capabilities, which had to be met by us for the sensors to be deployed. This was done by leveraging knowledge of experts in non-destructive testing, composite materials, additive manufacturing, which resulted in sensors that were manufactured with low-cost technologies such as screen printing, yet were rugged and are able to provide meaningful data throughout the service life of a composite. The next two chapters detail how we developed several iterations of eddy current sensors to gradually answer all those requirements.

In Chapter 2 we proposed the first iteration of our embedded sensors which was able to successfully measure ply migration, a critical manufacturing defect in CFRP, to 0.3mm accuracy. Additionally, characterization to validate that the embedded sensors did not impact composite structural integrity was conducted. This chapter represented an initial proof of concept for this next generation sensors, and required lots of synthetizing and distilling new learnings to make sure only the most pertinent parts were published.

Chapter 3 presents the subsequent generation of sensors, which thanks to new designs and architectures was able to measure strain and damage, in addition to previous functions. Furthermore, we look into the impact of substrate and encapsulation of embedded sensors, and found out that the thinner the substrate, the better the damage and strain sensitivity was for the sensor. As well as the fact that encapsulation prevented damage and strain from registering during stress testing, validating the fact that it was the matrix damage that was being measured instead of the deformation of the sensor material.

1.5 References

[1] [1] B. Ashrafi, M. B. Jakubinek, Y. Martinez-Rubi, M. Rahmat, D. Djokic, K. Laqua, D. Park, K.-S. Kim, B. Simard, A. Yousefpour, Acta astronautica 2017, 141, 57.

[2] R. M. A. Khan, I. E. Tabrizi, H. Q. Ali, E. Demir, M. Yildiz, Polymer testing 2020, 90, 106653.

[3] M. H. Lapena, C. M. A. Lopes, Plasma Processes & Polymers 2023, 20, 2200081.

[4] M. Rahmat, P. Hubert, Composites Science and Technology 2011, 72, 72.

[5] S. Erland, T. J. Dodwell, R. Butler, Composites. Part A, Applied science and manufacturing 2015, 77, 210.

[6] J. Guan, B. Ashrafi, Y. Martinez-Rubi, M. B. Jakubinek, M. Rahmat, K. S. Kim, B. Simard, Nanocomposites 2018, 4, 10.

[7] M. Rahmat, M. B. Jakubinek, B. Ashrafi, Y. Martinez-Rubi, B. Simard, ACS Omega 2022, 7, 10674.

[8] A. V. Skolunov, M. L. Marakhovskaya, M. V. Zhudenkov, Y. A. Blagodarov, M. E. Kazakov, Fibre Chem 2000, 32, 69.

[9] X. Wu, M. R. Wisnom, Composite Structures 2023, 304, 116467.

[10] J. S. Chilles, A. F. Koutsomitopoulou, A. J. Croxford, I. P. Bond, Composites Science and Technology 2016, 134, 81.

[11] A. H. Kalhori, W. S. Kim, ACS Appl. Electron. Mater. 2023, 5, 1.

[12] X. Liu, D. Li, H. Fukutani, P. Trudeau, L. Khoun, O. Mozenson, K. L. Sampson, M. Gallerneault, C. Paquet, T. Lacelle, B. Deore, O. Ferrand, J. Ferrigno, P. R. L. Malenfant, A. J. Kell, Adv Elect Materials 2021, 7, 2100194.

[13] A. J. Kell, C. Paquet, O. Mozenson, I. Djavani-Tabrizi, B. Deore, X. Liu, G. P. Lopinski, R. James, K. Hettak, J. Shaker, A. Momciu, J. Ferrigno, O. Ferrand, J. X. Hu, S. Lafrenière, P. R. L. Malenfant, ACS applied materials & interfaces 2017, 9, 17226.

[14] A. J. Kell, K. Wagner, X. Liu, B. H. Lessard, C. Paquet, ACS applied electronic materials 2024, 6, 1.

[15] H. Liao, X. Guo, P. Wan, G. Yu, Adv Funct Materials 2019, 29, 1904507.

[16] R. Toivola, S.-H. Jang, S. Baker, A. Jen, B. Flinn, Sensors 2018, 18, 1362.

[17] A. Winkler, N. Modler, W.-G. Drossel, T. Mäder, C. Körner, Advanced Engineering Materials 2018, 20, 1801001.

[18] A. Winkler, N. Modler, T. Weber, O. Täger, Advanced Engineering Materials 2018, 20, 1800588.

[19] L. Hou, S. A. Hayes, Smart Mater. Struct. 2002, 11, 966.

[20] C. Yan, J. Wang, W. Kang, M. Cui, X. Wang, C. Y. Foo, K. J. Chee, P. S. Lee, Advanced Materials 2014, 26, 2022.

[21] S. Tumanski, Meas. Sci. Technol. 2007, 18, R31.

[22] Z. Li, A. D. Haigh, M. N. Saleh, E. D. McCarthy, C. Soutis, A. A. P. Gibson, R. Sloan, Research in Nondestructive Evaluation 2018, 29, 123.

[23] X. Li, Z. Yang, X. Chen, Sensors 2014, 14, 7312.

[24] C. Huang, Y. Yao, V. Montes-García, M. Stoeckel, M. Von Holst, A. Ciesielski, P. Samorì, Small 2021, 17, 2007593.

[25] X. Zhao, Y. Zhang, W. Zhang, Z. Li, L. Kong, L. Yu, J. Ge, T. Yan, Optics & Laser Technology 2020, 124, 105997.

[26] R. de Oliveira, C. A. Ramos, A. T. Marques, Computers & Structures 2008, 86, 340.

[27] J. A. Etches, G. F. Fernando, Polymer Composites 2009, 30, 1265.

[28] O. Frazão, R. Oliveira, I. Dias, Microwave and Optical Technology Letters 2009, 51, 235.

[29] T. Karagiannis, E. F. Karachalios, N. D. Alexopoulos, Material Design & Processing Communications 2021, 3, e191.

[30] J. Missinne, N. Teigell Benéitez, A. Lamberti, G. Chiesura, G. Luyckx, M.-A. Mattelin, W. Van Paepegem, G. Van Steenberge, Advanced Engineering Materials 2018, 20, 1701127.

[31] M. Huang, L. Ding, W. Li, C.-Y. Chen, Z. Liu, IEEE Transactions on Circuits and Systems I: Regular Papers 2021, 68, 1659.

[32] N. Schmidová, J. Macken, A. Horoschenkoff, R. Sedláček, T. Kostroun, J. Šimota, M. Růžička, Applied Sciences 2022, 12, 1112.

[33] A. F. Carvalho, A. J. S. Fernandes, C. Leitão, J. Deuermeier, A. C. Marques, R. Martins, E. Fortunato, F. M. Costa, Adv Funct Materials 2018, 28, 1805271.

[34] A. Huijer, C. Kassapoglou, L. Pahlavan, Sensors 2021, 21, DOI 10.3390/s21206926.

[35] I. Read, P. Foote, S. Murray, Meas. Sci. Technol. 2002, 13, N5.

[36] B. Salski, W. Gwarek, P. Kopyt, P. Theodorakeas, I. Hatziioannidis, M. Koui, A. Y. B. Chong, S. M. Tan, V. Kappatos, C. Selcuk, T. H. Gan, J Nondestruct Eval 2016, 35, 25.

[37] T. Wang, D. Wu, W. Chen, J. Yang, Composite Structures 2021, 268, 114012.

[38] J. Barragán, A. Kell, X. Liu, S. Shin, C. Mandache, D. Djokic, D. Bennett, K. Houlahan, M. Genest, B. H. Lessard, C. Paquet, Adv Eng Mater 2025, 27, 2401332.

2. Next-Generation Embedded Printed Sensors for Near-Field Monitoring of High-Performance Composites

This chapter was published in the journal Advanced Engineering Materials: Barragán, J., Kell, A., Liu, X., Shin, S., Mandache, C., Djokic, D., Bennett, D., Houlahan, K., Genest, M., Lessard, B.H. and Paquet, C. (2025), Next-Generation Embedded Printed Sensors for Near-Field Monitoring of High-Performance Composites. Adv. Eng. Mater., 27: 2401332. https://doi.org/10.1002/adem.202401332

2.1 Context

This paper marked the first publication following our development of a proof of concept for embeddable sensors that measure ply migration. It synthetized a significant amount of learnings, from the creation of entirely new methodologies to the adaptation of existing characterization techniques for this novel application. Both the technology and the implementation methods were developed from the ground up when I started my masters. More specifically, the ink required testing and optimization, as did the sensor architecture, and the eddy current analysis tool settings. Once these components were refined and yielded meaningful data, each sensor was manufactured in triplicate, to establish standard deviations in testing, and subsequently embedded within composite laminates. Scans were conducted at each manufacturing step to measure their performance. Lastly, x-ray and CT scans were performed on the samples in order to show proof that the embedded sensors did not in fact result in any manufacturing defects.

Publication of this first work required considerable time and effort to reduce the large learnings from the experimental work into the most relevant information for the paper.

2.2 Contributions

This paper had the invaluable contributions of 2 research groups of the NRC in the research phase: the Quantum and Nanotechnology Research Centre provided help developing the inks and the treatment after printing (Kell, Liu, Shin), the Aerospace Research Centre (Genest, Djokic, Mandache) helped with training and guidance on EC scanning, as well as the embedding of the sensors in the composite. During writing, Dr Paquet and Dr Lessard helped streamline and define what would be published on the paper. During revision, Dayna Bennett and Katherine Houlahan from the NRC helped with micro-CT imaging. And finally, throughout the project, Dr Paquet helped with mentoring, planning of experiments, structuring of data, and general advice on the project.

2.3 Abstract:

Monitoring the structural health of composites during manufacturing and in-service is desirable to alert against damage or deterioration of conditions beyond an acceptable level. Wireless sensors embedded into materials that can endure the forming and curing of carbon fiber-reinforced polymer laminates will open the door to automated near-field detection of key metrics such as temperature, strain, and manufacturing defects. Current sensing technologies are generally too intrusive and fragile to be reliably embedded into laminates or too expensive to be applied commercially. The development of embedded, low-weight, small-footprint sensors is reported here, and how these sensors can be used to monitor ply movement during the manufacturing process is demonstrated. These screen-printed sensors consist of closed-loop spiral coils excited externally with an AC magnetic field to generate a secondary field, which alerts on the change of relative position of each ply. This proof-of-concept work demonstrates how printed coil sensors

can be fabricated to generate a high electromagnetic response, while minimizing their footprint in the laminate. It is determined that stacked silver coils, which are subsequently plated with copper to increase the conductance, are capable of producing signals that can be detected through over 3 mm of composite material.

2.4 Introduction

Carbon fiber-reinforced polymers (CFRP) are widely used as structural materials in aerospace, automotive, and naval sectors, to reduce vehicle weight and fuel consumption. This is mainly due to their superior specific strength and stiffness properties. Most commonly, these parts are made manually by sequentially laying up carbon fiber preimpregnated in thermosetting matrix (prepreg) plies over shaped tools and curing them in autoclaves.[1] One attractive processing improvement over this complex and error-prone process is forming, where the flat preforms are first assembled offline and then formed into complex 3D shapes, as defined by the mold geometry. Unlike metal forming processes, which involve plastic deformation of homogeneous materials, composite forming relies on inducing targeted inter- and inner-ply-slip. However, this is a sensitive process, and if not conducted properly, it can cause a range of adverse effects, such as corner thickening/thinning or ply wrinkling, which compromises the structural integrity of the part. These defects are difficult to mitigate due to challenges in detecting and predicting how these evolve during forming. Hence, sensing relative ply motion is key to understanding and avoiding the formation of defects. Postmanufacturing, the composite material will also endure thermal and mechanical stresses throughout its life cycle. To enhance the performance of the next-generation composite materials, wireless sensors that function with common nondestructive evaluation technologies could be easily embedded into laminates.[2]

Sensors, once seamlessly embedded into a CFRP part, can allow for strict control and verification of its condition or enable advancements in laminate technology. They can be used to monitor the health of the composite material and alert to the presence of matrix microcracks, delamination, and other critical defects.[3-12] They can also be used to monitor vibrations[13] or strains in material, statically or dynamically.[5, 14-18]

Current embedded sensor technologies used to monitor the health of CFRP and similar composite materials suffer from poor durability and are vulnerable to temperature changes experienced during manufacturing and throughout their life cycle. For example, fiber Bragg grating (FBG) (fiber optic based) sensors have elevated costs and are complex to develop, and their measurements can be compromised by temperature changes and require additional hardware, while also being difficult to maintain.[14, 19, 20] Piezoresistive material-based sensors can be depolarized at the high temperatures used during the manufacturing process of CFRP, have poor homogeneity in manufacturing, and may fail when facing stresses and conditions that are inherent to aerospace materials.[4, 9, 13, 21] Even more advanced systems, which combine both FBG and piezoresistive materials, can be used for damage detection. However, they still require complex electronics, expensive materials, and advanced algorithms, making them difficult to implement at larger scales. Nonetheless, they can achieve position accuracies between 5 and 25 mm for damage detection.[22]

Furthermore, once embedded they all have dimensions commensurate or larger than those within the defect inclusion threshold of 161 mm^2, which means that if used for commercial applications the composite piece would be considered defective.[9] Similarly, there are several innovations in the field of printed electronics integrated with CFRP. They vary greatly in application, from deicing on unmanned air vehicle (UAV) wings,[23] to damage detection using

printed copper and silver electrodes.[24, 25] However, these breakthroughs can only be applied to the surface of the CFRP, leaving it vulnerable to weather erosion, in addition to requiring the buffing of the top layer of epoxy in order to adhere correctly, thereby damaging the surface. To summarize, printed electronics usually only focus on the CFRP at a surface level, whereas embedded technologies can give better insight but tend to reduce the CFRP performance and entail additional cost or weight. Therein lies the novelty of the presented research, which combines the superior insight of fiber optic-based solutions, the simplicity of printed electronics, and importantly with minimal to no penalty to the structural integrity of the composite.

To better monitor the state of CFRP, a new system must be developed. The monitoring system requires the following: ability to accurately indicate ply position (from which ply migration can be inferred), not be invasive (i.e., not affect ply behavior, be compatible with the forming process, and be small enough to not be considered an inclusion), able to provide continuous measurements, be durable (survive forming, curing, and other post-processes), and able to provide qualitative and quantitative data. Printable sensors present an attractive solution to the sensors, as they could be wirelessly read, are inexpensive to manufacture, and fall below the threshold size of an inclusion.

Printed conductive coils that are embedded at critical locations within various layers of the composite materials have the ability to act as inexpensive and effective near-field sensors. The coils generate a magnetic field when externally stimulated, which can be remotely detected.[26] The detected field can provide information regarding the relative position of the sensor, temperature, or strain. Eddy current technologies, an industry-standard technology for nondestructive testing, could be leveraged for this purpose. The technique is based on electromagnetic induction and can detect very small defects in metals.[27-29] Therefore, this commonly used nondestructive evaluation

method, if applied to the detection of embedded sensors within a composite, would result in a reduced need for new testing equipment and training requirements. Using this detection technology, the electromagnetic response of the sensor can be measured periodically throughout the life of the composite material (a much less conductive medium than the sensors) to monitor its structural health. Effective sensors should have the following features: 1) coils that are tightly wound, with minimal turns to ensure the sensors have a small footprint and minimize their invasiveness within the laminate; 2) high electrical conductance to generate a sufficiently strong signal to be detected through the composite and at a given standoff distance; and 3) sufficient durability to withstand the process of forming and curing.

In this study, we report the design and optimization of screen-printed sensors that have high signal output, survivability to the forming and curing conditions, minimal physical area, height, and weight, resulting in minimal impact on the laminate behavior and integrity. Furthermore, the usage of screen printing, an inexpensive manufacturing method, would allow for commercial production at larger scales. We also describe the material architectures of ply sensors that can generate sufficient magnetic responses for wireless monitoring using eddy current technologies. The method uses screen-printed molecular silver inks that have high printing resolution and low film thickness ensuring the sensors maintain a small footprint within the laminate.[30] The material architectures are developed to increase the electrical performance amplifying the sensor sensitivity. Using real forming and curing trials, we demonstrate the sensors maintain their properties and provide location data with an accuracy higher than 0.25 mm. The approach to sensing has been optimized and opens the opportunity to further miniaturize the sensors and increase performance. The proposed work here is unique, as it puts forward a new approach to noncontact and in situ

monitoring of CFRP manufacturing, and it paves the way for printed embedded sensors in structural health monitoring using convenient nondestructive techniques.

2.5 Results and Discussion

The experimental procedure uses CFRP-embedded planar spiral coils excited and sensed via electromagnetic induction with a transmit–receive eddy current probe scanning the composite part. **Figure** 7a shows the experimental setup of the EC NDT equipment, with the bottom representing the coil and the top representing the inductor. Their signal strength increases with the number of turns in a coil.[27] Therefore, to ensure the sensors maintain a small footprint and generate a signal that could be detected through the composite with at least a 3 mm standoff distance, the coils were designed to have tightly wound turns. We found coils with nominal line width of 300 μm and line spacing of 100 μm afforded sensors with a high turn density without causing adjacent lines of the coil to short as a result of ink slumping.

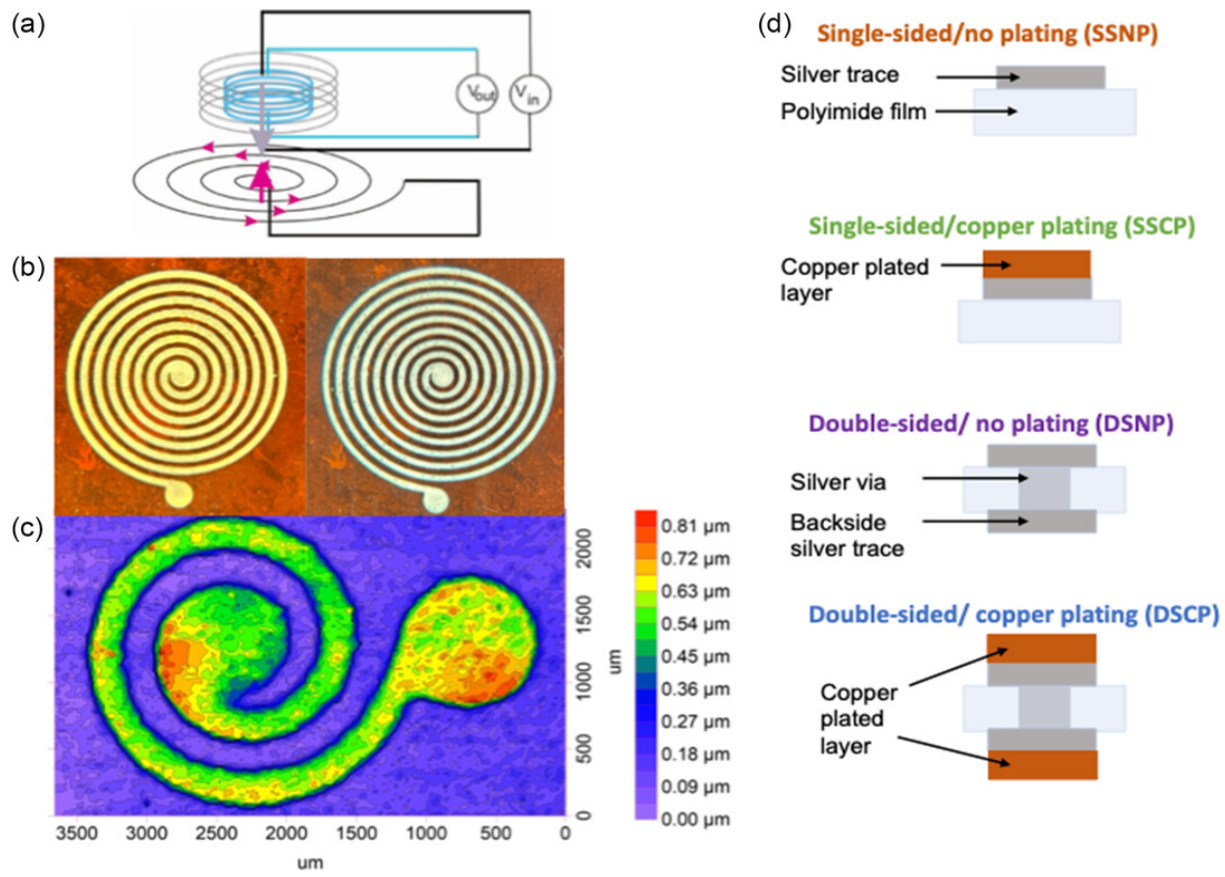

Figure 7*: a) EC testing setup: Probe has signal reading (gray) and emitting (blue) components to measure the output (pink) from the spiral sensor. b) 7- and 8-turn non-plated sensor. c) Topography of a 1-turn sensor. d) Proposed architectures for spiral sensors.*

A set of coils were designed with varying numbers of turns, ranging from 1 turn (at 1.78 cm in linear length and 2 mm in diameter) to 9 turns (16.76 cm in linear length and 10 mm in diameter) with constant nominal line width and line spacing. Figure 7b shows a coil design with 7 and 8 turns, and Figure 7c shows the topography of a 1-turn sensor; in practice, it is slightly more than 1 turn, but for the purposes of this work, turns are defined as the number of lines between the base and the center. The baseline sensor architecture consisted of coils printed with silver molecular ink on polyimide film and is referred to as a single-sided nonplated sensor (SSNP). In addition to this sensor structure, three other sensor architectures were explored, as illustrated in Figure 7d. The

baseline sensor, SSNP, was copper plated for 120 min yielding single-sided copper-plated (SSCP) sensors. Alternatively, coils were printed on both sides of the substrate to obtain a higher turn density for an identical size, producing double-sided nonplated (DSNP) sensors. Lastly, a combination of the former and latter approaches was used to yield double-sided copper-plated (DSCP) sensors.

The signal output from these sensors will be governed by the overall conductance and number of turns per coil. Low resistivity and low resistance (i.e., high conductance) traces are desirable because they would allow a higher induced current to flow through their turns. Despite the low volume resistivity that can be achieved with silver traces, the method of screen-printing limits how much ink can be deposited and therefore sets an upper limit on the thickness of the silver trace, capping the achievable conductance. Increases in the trace thickness would significantly improve the sensor performance with only marginally increasing the total volume of the sensor. Copper electroless plating was used as a means to increase the trace thickness and conductance to improve the sensor performance. Copper plating is particularly attractive as it deposits metal over top of the silver seed layer with limited growth laterally and therefore would not cause the lines to widen and shorten. In this work, the amount of copper deposited to the traces was tuned by controlling the plating time, offering a way to balance the quality of the sensors with conductance. The amount of copper deposited in a given time period depends on the solution and can range from 5 $\mu m\, h^{-1}$ for certain commercial products to 8 $\mu m\, h^{-1}$ for high-concentration solutions.[31] The copper plating solution used in this work had low concentrations of precursors, depositing at a low rate of 0.32 $\mu m\, h^{-1}$ and ensuring a uniform copper film formed. Coils were plated for 30, 60, and 120 min. Above 120 min of plating, the quality of plated copper degraded. **Figure 8**a shows the profile of plated and nonplated traces and confirms that the copper layer does

not grow laterally, maintaining similar trace widths. The silver traces were found to have average heights of 0.58 ± 0.06 µm. Following 20 min of copper plating, the height of the coils increases to at least 1.5 µm from the initial 0.6 µm. Prior to copper plating, the silver traces had a volume resistivity of 90 µΩ cm, a value higher than that found in literature of 15–45 µΩ cm.[32] This difference is due to the higher content of polymer binder in the ink that was added to ensure the traces survive the copper plating process. Figure 8b also shows the significant decrease in resistance and volume resistivity with increasing plating times. The resistivity decreases to a value of 4.66 µΩ cm, about 2.7 times higher than pure copper (1.72 µΩ cm).[33]

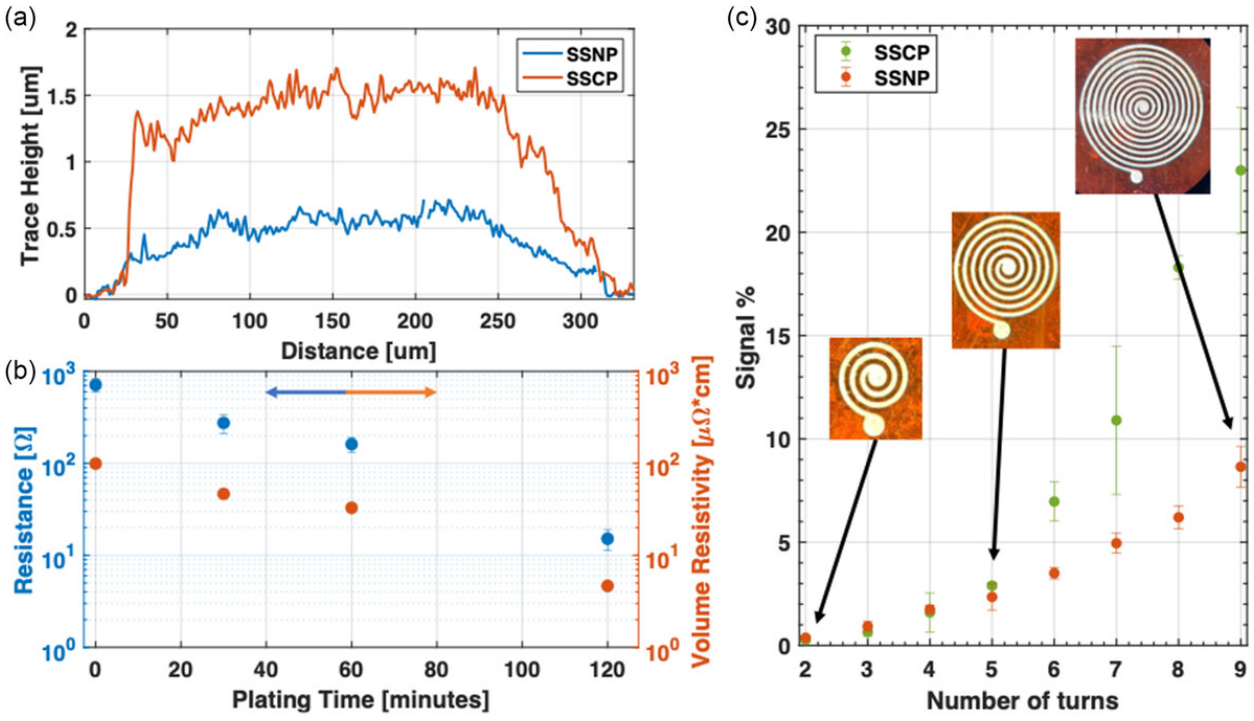

***Figure 8**: a) Height profile of traces from a silver- (SSNP) and copper-plated (SSCP) sensor. The copper plating increasing the thickness while keeping the width constant; b) changes in the traces resistance and volume resistivity with copper plating time; c) the signal readout of the sensors with different numbers of turns for copper-plated (SSCP) and noncopper-plated single-sided (SSNP) sensors (measurements were performed with a 1 mm stand-off between the sensors and the probe).*

The signal strength is predicted to increase with the number of turns[27] and with decreasing resistance (increasing conductance) of the traces. The dependence of the number of turns on the signal output was evaluated at a separation of 1 mm for sensor architectures SSNP and SSCP. The results, found in Figure 8c, reveal the tradeoff between the size or footprint of sensor and its signal strength, as previously shown by Ditchurn et al.[27] The signal readout increases exponentially with the number of turns/coil for both SSNP and SSCP sensors. For instance, the 5-turn SSNP sensor has a signal of around 2% while the 9-turn sensor has a signal of 8.65%. Copper plating is shown to further improve sensor performance, as shown in the signal enhancement for the SSCP series. The relative improvement imparted by copper plating increases with the number of turns in the sensor. In this case, the 5-turn sensor has a signal of 3% (a relative 50% increase over the SSNP analog) while the 9-turn sensor has a readout of 23% (or a relative 266% increase over the SSNP analog). The significant tradeoff between sensor performance and footprint is especially important as large sensors can compromise the structural integrity of the composite.

Using sensors with 9 turns (10 mm in diameter), the different architectures (SSNP, SSCP, DSNP, and DSCP) were compared. As shown in **Figure 9**a, the sensor architecture has a strong impact on signal output. As mentioned in the experimental section, the signal output percentage consists of the ratio between energy emitted and recovered by the probe. For instance, the SSNP, SSCP, DSNP, and DSCP had signal outputs of 17.5, 30.3, 34.0, and 56.3% respectively, demonstrating that the signal for the sensors with the DSCP architecture is around 4 times higher than the SSNP. Additionally, the copper-plated (SSCP) and the double-side sensor with no copper plating (DSNP) show statistically identical increases in performance for the sensor, ≈2 times the baseline (SSNP) sensor. The DSCP sensors outperform all other sensor architectures highlighting how copper plating and stacking coils by printing on two sides of the substrates can be combined

to significantly boost the signal output without significantly increasing the size of the sensors (i.e., increase in thickness of about 1 µm compared to the 50 µm thickness of the polyimide film).

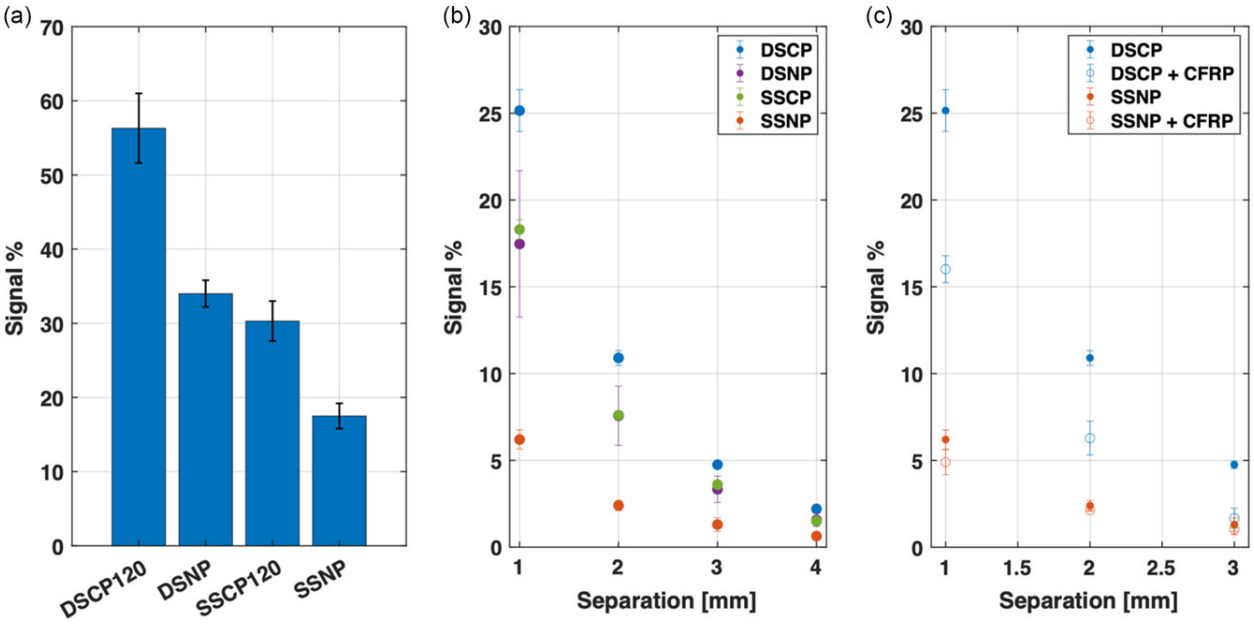

Figure 9: *a) Signal readout for 9-turn sensors with different architectures measured at 0 mm between the probe and the sensor. b) Signal readout for 9-turn sensors with different architectures from 1 to 4 mm distances between the probe and the sensor. c) Signal readout for 9-turn sensors with different architectures with a piece of CFRP with thicknesses of 1–3 mm.*

The signal strength is predicted to decrease exponentially with distance,[34] underlying the need for efficient sensors to monitor through thick laminates or at large standoff distances. Therefore, these sensors were also evaluated at separation distances ranging from 1 to 4 mm from the measurement probe. This measurement is critical given that one of the objectives for this study is to obtain a readable signal from at least 3 mm separation. Results for this measurement are found in Figure 9b and confirm that the signal decreases exponentially as separation from the sensor increases as predicted by Tumanski.[34] Despite the exponential decrease in signal, all architectures remain readable at 4 mm stand-off from the coil's plane. The DSCP has the highest performance due to the implementation of both signal-enhancing techniques (more turns and lowest resistance).

Three key trends of sensor behavior can be established from this data: (1) high number of turns per coil and lower resistance resulted in a higher signal output; 2) features of the sensor architectures can be combined to create a very high-performing sensor; and 3) the signal had an exponential decrease as separation from the probe increased.

Before embedding sensors into laminates, the impact of the CFRP laminate layer on them was investigated. Because there is no precedent for the extent to which CFRP decreases the signal for passive sensors of this kind (making the obtained measurements even more critical for future near-field sensors of similar architectures), the baseline SSNP sensor and the top-performing architecture, DSCP, with 9 turns were measured at different distances, with and without a CFRP sheet of a width equal to the separation distance placed in between the probe and the sensor. Figure 9c shows the results of the measurements, which found that dampening can vary between 30 and 60% in comparison to air and was much more noticeable for the better-performing sensor. This dampening is consistent with the fact that CFRP acts as a shielding layer with resistivity of 0.022 and 310 mΩ m along and across the fibers respectively.[35] Despite the reduction in signal, the sensors still have sufficiently strong signal output to be embedded into the laminates. For instance, at 3 mm standoff distance, the DSCP sensor had its 4.75% signal strength reduced to ≈2% with the CFRP panel above it.

For the forming and curing trials, four 9-turn SSNP sensors were embedded in a CFRP test part to test the survivability and performance of the sensors. **Figure 10**a shows the three stages of the process in which the CFRP piece was scanned: 1) laminate, where the plies are assembled into a flat preform and the sensors embedded; 2) forming, where the preform is deformed to a desired shape with application of external heat and force; and 3) curing, where the piece is heated up in an autoclave and becomes rigid. An eddy current scan of the piece was taken at each step to compare

the position of the embedded sensors and to verify that the sensor remains functional during harsh manufacturing conditions. The sensors were placed between plies of a preimpregnated sheet at various depths, with 3 additional sensors embedded at static positions to serve as references (R1, R2, and R3P1D). Figure S3 and S4, Supporting Information, show the structural spar that was embedded with the sensors. Figure 10b shows the superimposed scanned position of the 4 sensors at each step, with red, blue, and green representing the uncured, formed, and cured manufacturing steps, respectively. The sensors (9-turn coils, SSNP architecture) labeled A, B, C, and D were embedded at depths ranging from 0.135 up to 3.375 mm, with more displacement expected at shallower depths due to the geometry of the formed CFRP piece. The black square below the schematic represents the scanned surface and shows the displacement of the sensors at a millimeter scale. Figure S5, Supporting Information, presents a more visual representation of the ply migration during forming. Figure 10c shows the displacement of each sensor as a function of their embedding depth. The experimental results were compared with the theoretical displacement expected out of each ply and show an accuracy of ±0.6 mm (represented by the error bar), which could be further decreased to ±0.15 mm (the minimum step of the probe) with additional scans, though precision optimization was beyond the scope of this article. Whereas this technique is less accurate than X-ray equipment, which can have resolutions down to 0.015–0.2 mm,[36] it does not require embedding metal wires into the composite (which affects the structural integrity) nor specialized and expensive X-ray equipment. In contrast, EC NDT equipment is readily available and already used for other testing such as turbine blade damage[37] and would just require a change of settings in order to be able to read the sensors correctly.

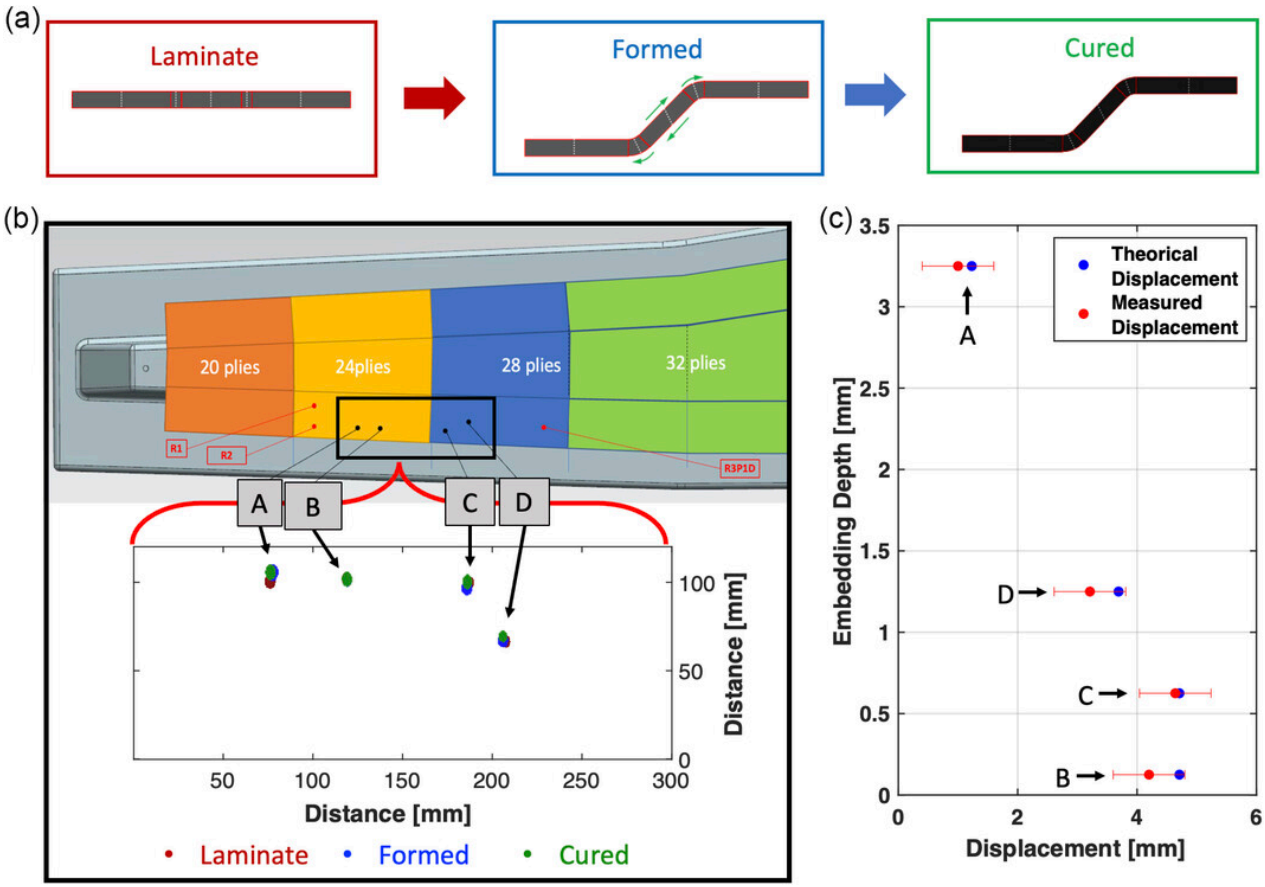

Figure 10: *a) Illustration of a CFRP laminate cross section at different manufacturing stages, showing possible ply migration with green arrows. b) Schematic showing the lateral location of four 9-turn SSNP sensors, each represented by a letter (top) and the superimposed scans of the sensors within the CFRP part as their location changes throughout the different manufacturing steps (the locations of the sensors in the top schematic are mirrored in the bottom plot). c) Quantitative analysis comparing the algebraically calculated and the experimentally measured displacement for each marker.*

Having validated the performance of the sensors, they could be used to inform on possible ply defects if the theoretical displacement does not fall within the error of the measured displacement. A digital rendering of the composite and where the sensors are embedded can be seen in Figure S3, Supporting Information. This last figure demonstrates that the proposed sensors

can undergo forming and curing of a CFRP piece, while retaining functionality, and yielding valuable information about the relative displacement of plies. These location sensors illustrate the potential for advanced and automated wireless monitoring using seamlessly integrated sensors into composites.

The sensors were covered with 25 µm polyimide tape before embedding to ensure the sensors did not adhere to CFRP and the copper layer and silver trace were not affected by the changes in CFRP. Since the embedded sensors fall below the inclusion size threshold at which structural integrity would be significantly affected by delamination (under 2.5% decrease in compressive strength for delamination smaller than 100 mm^2),[38] the embedded sensors were assumed to have little to no impact on the structural performance of the composite.

Sections of the CFRP containing the embedded sensors were cut in half and imaged using an X-ray and an optical microscope to verify no delamination or defects were present. **Figure 11**a,b shows the cross section of a 7-turn SSNP sensor embedded in CFRP taken with an optical microscope, after cutting the sample in half and polishing it. The embedded sensor can be clearly seen as the dark gray layer in Figure 11a, with the different orientation plies of CFRP showing as lighter layers. The interface between each layer can be seen in Figure 11b; no delamination and minimal defects could be observed between the encapsulating 25 µm polyimide film and the CFRP. The thicker polyimide substrate can be seen at the center of the image, and the coils can be faintly observed in between the thin polyimide wrapping and the thicker substrate. To better observe the coils and any other possible defects, micro-CT X-ray images (Figure 11c,d) were taken. Figure 11c shows the cross section of the cut sensor, the coils can be observed as bright orange lines, the polyimide substrate can be seen in the darker purple areas in between the coils as well as extending

slightly past them, since some margin of the substrate was left to avoid damaging the coils. Figure 11d shows the top view of the cut sensor.

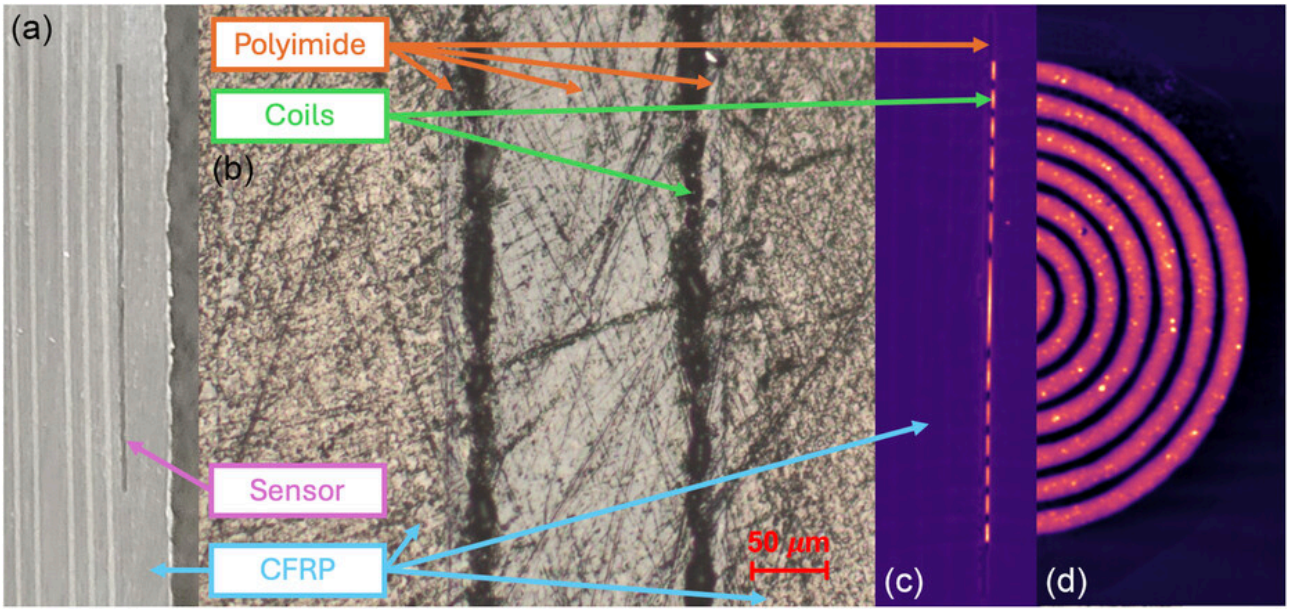

Figure 11: *a) Photograph of a cross section of a 7-turn SSNP sensor embedded in composite; b) cross section of a 7-turn SSNP sensor with 20× optical magnification showing 4 distinct layers (from left to right: CFRP—1 mil polyimide wrapping—polyimide substrate—coils—1 mil polyimide wrapping—CFRP); c) cross section of a micro-CT scan of a 7-turn SSNP sensor, with the coils showing in orange, the polyimide substrate in dark purple and the CFRP in lighter purple; d) top view slice of a micro-CT image of the 7-turn SSNP sensor shown in 11c.*

Furthermore, it was found that a 9-turn SSNP sensor (the largest manufactured) was 42.5 mg, out of which the polyimide substrate accounted for 42.0 mg. CFRP has a density of 1.6 g cm^{-3};[39] therefore, a 1 m^2 piece of 4 mm thickness would be around 6.4 kg. Assuming a very high sensor load of 34 (1 per ply and 4 references), their total weight would be of 1.4 g, less than 0.02% of the piece weight. This could be reduced by around 99%, or 1.383 g, if the polyimide substrate was removed highlighting the importance of developing directly printable technologies. In any case, as the weight of sensors is below 0.02% their weight penalty on the piece can be assumed negligible.

2.6 Conclusion

A proof of concept for novel passive electromagnetic sensors to be manufactured via the inexpensive and scalable method of screen printing was presented. The printed conductive coils generate a magnetic field when externally excited, allowing for near-field sensing. Various material architectures were evaluated and led to the identification of a sensor platform that has a small footprint, high durability, and performance, as well as good survivability to high temperatures and low pressure used during the curing and forming of CFRP. It was demonstrated that double-sided printing and copper plating increase the signal output, and the combination of both techniques can result in a signal five times larger than that of a control sensor without those enhancements. The manufactured sensors provided valuable insight into ply migration, which was tested by embedding them into primary structural component for aerospace applications. We achieved an accuracy of over 0.6 mm when measuring ply migration, with the ability to read through over 3 mm of CFRP, with sensors varying from 1 to 9 turns, and ranging from 0.5 to 1.5 μm in thickness, depending on the architecture used. Furthermore, accuracy and improvements could be attained with optimized coil shapes and advanced post-processing image analysis. Lastly, the CFRP pieces were cut in half and the cross section of the embedded sensors was scrutinized with optical microscopy and X-ray imaging, revealing no delamination as well as minimal defects.

Future work will involve optimizing sensor accuracy in order to bring it down to 0.15 mm (current testing equipment limit), embedding the sensor directly, without the need for any Kapton tape or polyimide film, and using the sensor for detection of damage in addition to ply migration monitoring.

2.7 Experimental Section

2.7.1 Screen Printing

Meshtech NBC[40] fabricated the screen with a coil pattern using photoimaged MM1 emulsion (10–14 μm) supported on an SS360 stainless steel mesh. The method to prepare and print silver molecular inks is described elsewhere;[32] the ink is based on silver neodecanoate combined with a polymeric binder, and with a final viscosity of between 5000 and 6000 cP. Polyimide film was chosen as a substrate for its compatibility with the processing conditions used in forming the CFRP, most importantly its chemical and thermal stability. Sensors were prepared by screen printing the molecular ink onto 21.6 cm × 27.9 cm sheets of polyimide film using a flatbed American M&M S-912M[41] small format screen printer.

2.7.2 Post-printing Processing

The silver traces were processed following the methods from Liu et al and Wagner et al.[42, 43] which consist of UV curing followed by thermal sintering. To connect both terminals of the sensor, small perforations were made through the polyimide film, and a thin and narrow silver ink trace was deposited with a syringe on the back of the substrate to complete the closed-loop spiral. Then, the curing and sintering process was repeated to make the back-trace conductive. For double-sided sensors, the coils were printed, UV cured, and sintered on both sides of the film, and then, the electrical connections between two coils were made simultaneously through substrate perforations at specific locations.

2.7.3 Copper Plating

For samples that were electrolessly plated with copper, the additional binder was used in the silver ink formulation in comparison to that described in an earlier report.[30, 32] The additional binder served to increase the adhesion of the metal trace to polyimide film, but also increased the

trace volume resistivity up to 90 μΩ cm from the literature value of 15–45 μΩ cm for pure silver sensors.[32] The silver sensors were submerged in an electroless plating solution for a given amount of time, as per Hibder et al.[44] The solution is based on CuSO4, Rochelle Salts, NaOH, and formaldehyde. Postplating, the sensors were removed from the copper plating solution, rinsed with distilled water, and dried with nitrogen. The copper plating decreased the resistivity of the baseline coils (silver only) by 20–30%. An optimal plating time of 120 min was determined in which sensors could be fabricated uniformly, with high trace thickness and good adhesion. Longer plating times resulted in defects, including flaking, where the trace separates from the substrate; increased surface roughness; copper depositing laterally causing coils to short; and delamination, which occurred when the entire trace separated. Three replicates of each architecture and size of sensor were made to account for manufacturing variances.

2.7.4 Characterization

The sensors were characterized using several techniques. A CT100 Cyber Technologies optical profilometer[45] was used to measure the height, thickness, and surface roughness of the printed sensors. A Bruker 1275 Skyscan X-ray[46] was used to verify any delamination or deformities that could have been caused by the sensor in the CFRP. A saw was used to cut the sample at the location of the sensor, yielding a cross section of the embedded sensor in the composite. Polish was used to ensure the cut surface was clean. Optical microscope images were taken using a ZEISS Stereo Discovery microscope.[47] A Fluke 115 Digital Multimeter with Pomona electronics 6341 tips[48] was used to measure the resistance between the center and the edge of the sensor before bridging both terminals together. The resistance was observed to increase proportionally to the number of turns in a sensor, varying from 4.7 Ω for the 2-turn sensor up to 37.2 Ω for the 9-turn sensor. Lastly, eddy current testing was done to validate performance. This

was done using an EC TecView Acquisition and Analysis software and hardware,[49] with a transmit-receive reflection type EC probe consisting of an outer excitation coil and an inner receiver. The frequency tuning of our three-coil (inductor, sensor, and receiver) system was determined experimentally and found to be in the range of 100–250 kHz; subsequently, we used a frequency of 200 kHz to drive the transmitter component of our eddy current probe. The probe was excited with a 200 kHz, 10 V_{pp} sinusoidal waveform, while a 40 dB gain was applied to the receiver signal. The probe was mounted in a robotic arm able to scan a planar (horizontal) test piece at a speed of 12 mm s^{-1}, and a step of 1 mm on both scanning and indexing directions. The measurements were taken at separations (on the vertical axis) varying from 1 up to 4 mm between the sensor's plane and the probe. In addition to the excitation coil, the scanning probe contains an inner, concentric coil, shielded from the excitation one which allows for the reading of the signal from the sensor. The voltage amplitude of the receiving coil is the output used for analysis. This amplitude is expressed as a percentage, based on the recorded orthogonal eddy current signal components, with 100% representing the maximum on a scale of 5 V_{pp}, after application of the gain settings. Since all instrument parameters were kept the same for all scans, the percentage amplitude value allows for quantitative comparison among various experiments.

To measure the effects of composite materials, eddy current scans were performed with sheets of CFRP of varying thicknesses (1, 2, 3, and 4 mm) placed on top of the printed sensors. Measurements were calibrated at a 0 mm separation distance between the probe and sensor followed by measurements taken with 1 mm incremental increases in separation up to 4 mm.

The sensors underwent forming and curing trials. They were embedded during the hand layup deposition of the prepreg plies for the manufacture of a flat preform. Before this, they were wrapped in 1 mil Kapton tape. A standard unidirectional carbon/epoxy composite prepreg

(0.135 mm thickness per ply) was used. During the placement of each sensor, the position was marked on a guide sheet to keep a record of its depth of embedment (from 0.135 to 4 mm). The laminates were formed into a desired 3D shape and then cured in an autoclave, at 6 bar, 177 °C for 5 h. Using the eddy current procedure described above, the sensors were interrogated after the preform fabrication, forming and curing steps. The data was then processed with VBA and MATLAB scripts in order to obtain the relative displacement of each sensor.

2.8 Supplementary Information

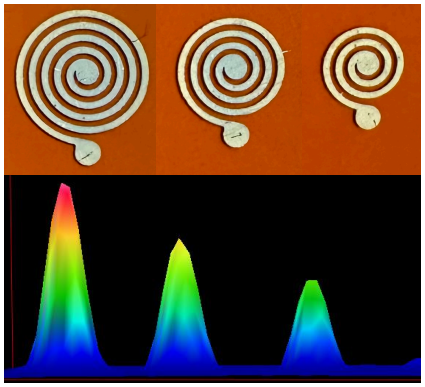

ESI S1*: EC Testing Scan of sensors of different architectures and sizes and SSNP sensors of 6 and 7 turns*

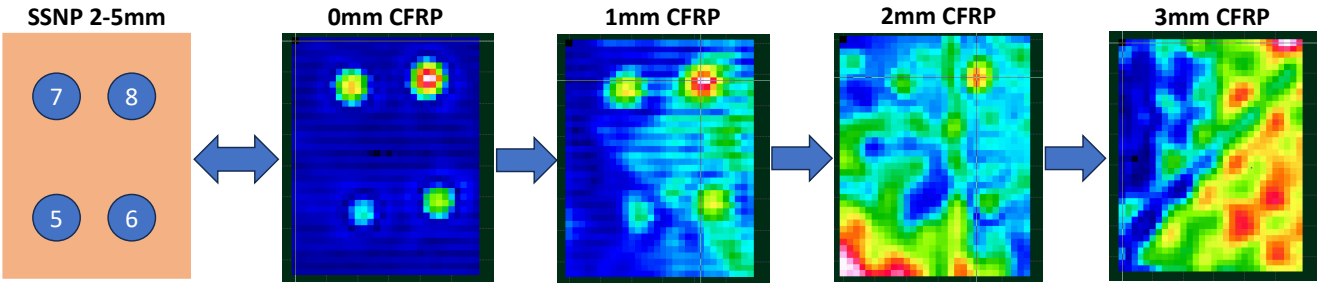

ESI S2*: Visualization CFRP EC signal shielding: 4 sensors of 5-8 turns with gradually thicker pieces CFRP placed on top of them demonstrate the increasing shielding effect.*

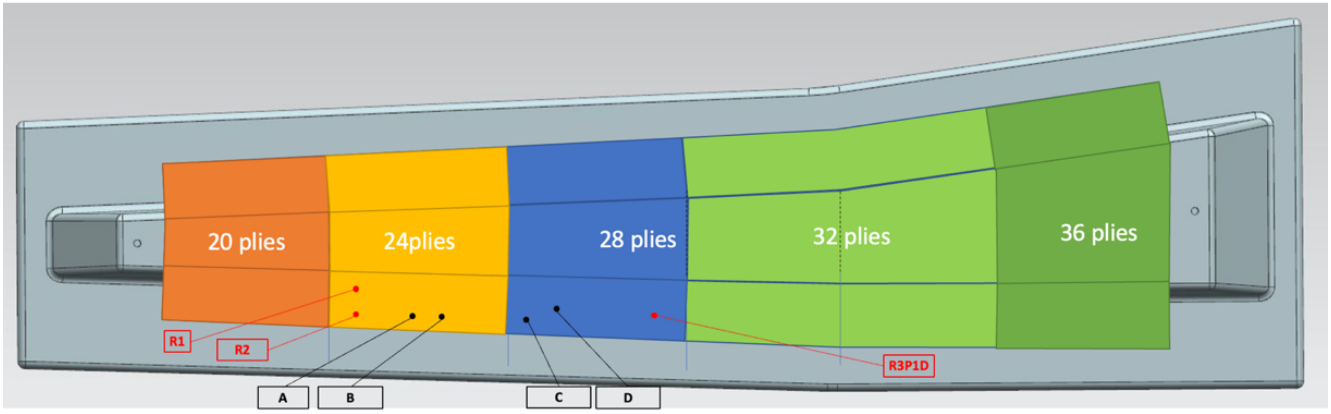

Code	Function	Expected sensor migration [mm]	Embedding depth [mm]
R1	Reference	0	3
R2	Reference	0	3
A	Ply location	1.23	3.125
B	Ply location	4.71	0.125
C	Ply location	4.71	0.625
D	Ply location	3.69	1.25
R3	Ply location	0	4

***ESI S3**: Digital rendering of CFRP piece, indicating where the sensors were embedded. Includes the 3 reference sensors as well as the 4 sensors used for ply migration.*

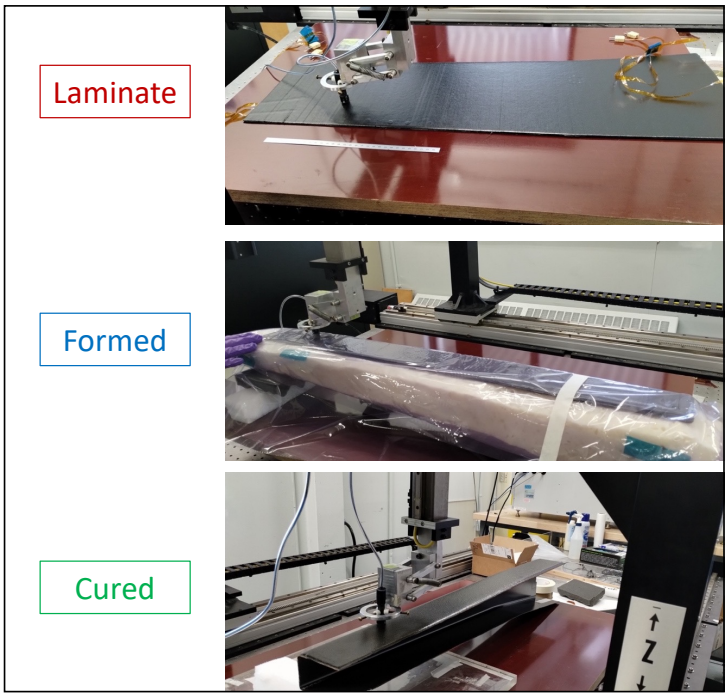

***ESI S4**: Pictures of the piece shown in S3 whilst being scanned by the EC equipment*

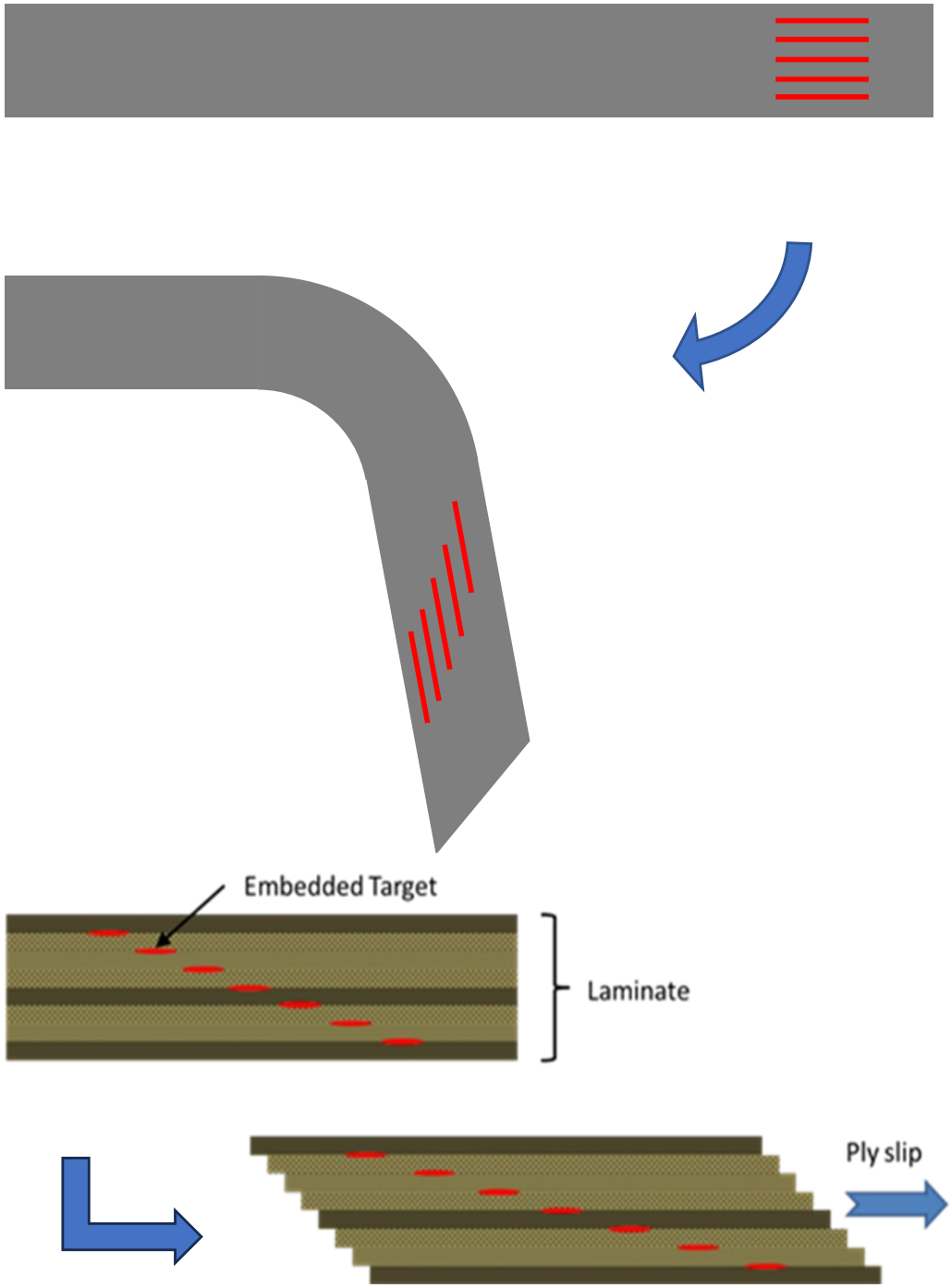

***ESI S5**: Visualization of sensors at different embedding depths, and how the plies migrate throughout the forming process.*

2.9 Acknowledgements

This research was supported by the Security and Disruptive Technologies division of the National Research Council Canada. Open Access funding provided by the National Research Council Canada library.

2.10 Conflict of Interest

The authors declare no conflict of interest.

2.11 References

[1] B. Ashrafi, M.B. Jakubinek, Y. Martinez-Rubi, M. Rahmat, D. Djokic, K. Laqua, D. Park, K.-S. Kim, B. Simard, A. Yousefpour, Acta Astronautica 2017, 141, 57.

[2] S. Erland, T.J. Dodwell, R. Butler, Composites. Part A, Applied Science and Manufacturing 2015, 77, 210.

[3] R.M.A. Khan, I.E. Tabrizi, H.Q. Ali, E. Demir, M. Yildiz, Polymer Testing 2020, 90, 106653.

[4] G. Mook, J. Pohl, F. Michel, T. Benziger, A. Hilbig, in Materials for Transportation Technology, 2000, 198.

[5] R. de Oliveira, C.A. Ramos, A.T. Marques, Computers & Structures 2008, 86, 340.

[6] A. Gullapalli, V. Beedasy, J.D.S. Vincent, Z. Leong, P. Smith, N. Morley, Advanced Engineering Materials 2021, 23, 2100313.

[7] J.S. Chilles, A.F. Koutsomitopoulou, A.J. Croxford, I.P. Bond, Composites Science and Technology 2016, 134, 81.

[8] A. Huijer, C. Kassapoglou, L. Pahlavan, Sensors 2021, 21.

[9] R. Janeliukstis, D. Mironovs, Mechanics of Composite Materials 2021, 57, 131.

[10] X. Cheng, X. Cao, Z. Wu, Z. Ying, D. Camilleri, X. Hu, Advanced Engineering Materials 2023, n/a.

[11] A. Winkler, N. Modler, W.-G. Drossel, T. Mäder, C. Körner, Advanced Engineering Materials 2018, 20, 1801001.

[12] Y. Lv, L. Min, F. Niu, Z. Qin, M. Zhang, B. Zhao, Y. Liu, K. Pan, Advanced Materials Technologies 2023, 8, 2201886.

[13] A. Winkler, N. Modler, T. Weber, O. Täger, Advanced Engineering Materials 2018, 20, 1800588.

[14] T. Karagiannis, E.F. Karachalios, N.D. Alexopoulos, Material Design & Processing Communications 2021, 3, e191.

[15] Ç. Yılmaz, H.Q. Ali, M. Yıldız, Polymer Composites 2023, 44, 2956.

[16] O. Frazão, R. Oliveira, I. Dias, Microwave and Optical Technology Letters 2009, 51, 235.

[17] J.A. Etches, G.F. Fernando, Polymer Composites 2009, 30, 1265.

[18] J.A. Etches, G.F. Fernando, Polymer Composites 2010, 31, 284.

[19] J. Missinne, N. Teigell Benéitez, A. Lamberti, G. Chiesura, G. Luyckx, M.-A. Mattelin, W. Van Paepegem, G. Van Steenberge, Advanced Engineering Materials 2018, 20, 1701127.

[20] M. Majumder, T.K. Gangopadhyay, A.K. Chakraborty, K. Dasgupta, D.K. Bhattacharya, Sensors and Actuators A: Physical 2008, 147, 150.

[21] S. Geller, T. Tyczynski, M. Gude, S. Sauer, W.-J. Fischer, Advanced Engineering Materials 2018, 20, 1800447.

[22] D. Barazanchy, M. Martinez, B. Rocha, M. Yanishevsky, Journal of Sensors 2014, 2014, 1.

[23] M.K. Idris, J. Qiu, G.W. Melenka, G. Grau, Eng. Res. Express 2020, 2, 025022.

[24] S.-J. Joo, M.-H. Yu, E.-B. Jeon, H.-S. Kim, Composites Science and Technology 2017, 142, 189.

[25] E.-B. Jeon, T. Fujimura, K. Takahashi, H.-S. Kim, Composites Part A: Applied Science and Manufacturing 2014, 66, 193.

[26] C. Mandache, R. Desnoyers, Y. Bombardier, Sensors 2022, 22.

[27] R.J. Ditchburn, S.K. Burke, NDT & E International : Independent Nondestructive Testing and Evaluation 2005, 38, 690.

[28] K. Koyama, H. Hoshikawa, G. Kojima, Journal of Pressure Vessel Technology 2013, 135, 041501.

[29] T. Wang, D. Wu, W. Chen, J. Yang, Composite Structures 2021, 268, 114012.

[30] A.J. Kell, K. Wagner, X. Liu, B.H. Lessard, C. Paquet, ACS Applied Electronic Materials 2024, 6, 1.

[31] NBC Meshtech Americas, 2023.

[32] A.J. Kell, C. Paquet, O. Mozenson, I. Djavani-Tabrizi, B. Deore, X. Liu, G.P. Lopinski, R. James, K. Hettak, J. Shaker, A. Momciu, J. Ferrigno, O. Ferrand, J.X. Hu, S. Lafrenière, P.R.L. Malenfant, ACS Applied Materials & Interfaces 2017, 9, 17226.

[33] Catspit Screen Print Supply, Catspit Screen Print Supply - Phoenix, Arizona 2023.

[34] K. Wagner, S. Zou, Y. Martinez-Rubi, A.J. Kell, C. Paquet, B.H. Lessard, FPE 2023, 8, 25005.

[35] X. Liu, D. Li, H. Fukutani, P. Trudeau, L. Khoun, O. Mozenson, K.L. Sampson, M. Gallerneault, C. Paquet, T. Lacelle, B. Deore, O. Ferrand, J. Ferrigno, P.R.L. Malenfant, A.J. Kell, Adv Elect Materials 2021, 7, 2100194.

[36] P.C. Hidber, P.F. Nealey, W. Helbig, G.M. Whitesides, Langmuir 1996, 12, 5209.

[37] Snowhouse 2024.

[38] Fluke, Fluke 2020.

[39] TecScan, 2023.

[40] J.H. Huang, P.S. Shih, V. Renganathan, S.J. Gräfner, Y.A. Chen, C.H. Huang, C.L. Kao, Y.S. Lin, Y.C. Hung, C.R. Kao, Electrochimica Acta 2022, 425, 140710.

[41] D.C. Giancoli, Physics Education 2000, 35, 370.

[42] S. Tumanski, Measurement Science & Technology 2007, 18, R31.

[43] N. Angelidis, C.Y. Wei, P.E. Irving, Composites Part A: Applied Science and Manufacturing 2004, 35, 1135.

[44] E. Dilonardo, M. Nacucchi, F. De Pascalis, M. Zarrelli, C. Giannini, Composites Science and Technology 2020, 192, 108093.

[45] T. Liang, W. Ren, G.Y. Tian, M. Elradi, Y. Gao, Composite Structures 2016, 143, 352.

[46] Y. Zhang, K. Huang, R. Sun, F. Liao, L. Guo, L. Zhang, Composite Structures 2022, 281, 115063.

[47] M.A. El-Reedy, in Asset Integrity Management for Offshore and Onshore Structures, Elsevier2022, 199.

3. Next generation embedded printed sensors for near-field monitoring of high-performance composites: Damage and Strain Measurement

This chapter is currently being formatted for publication submission.

3.1 Context

With all the groundwork on characterization and understanding of the technology from the previous paper, our next objective was to further develop the sensors in order to use them for damage and strain measurement in composites. With the initial establishment of ink, EC scanning settings, and post processing of the sensors, we could focus on sensor improvement through designs and architectures. Therefore, we explored new sensors (shorter coils, concentric rings, and discs), then optimized their architecture, finally deciding on multi-layer disc printing as the most advantageous solution. Then, new composite samples had to be designed and manufactured in order to be compatible with industry standard equipment for stress testing. Lastly, a new EC scanning setup had to be designed and optimized, as we previously used EC equipment that would only work for static tests, and wouldn't prove reliable for the dynamic tests ahead. The only remaining steps were to test out the embedded sensors in the newly designed composites and testing jig, as well as design a protocol for the stress testing.

3.2 Contributions

This paper had the invaluable contributions of Drazen Djokic, Dr Catalin Mandache, and Marc Genest in the design of the new EC testing setup, the new composite cutouts that would be compatible with the stress testing equipment, and the development of the protocol for stress testing. Marc Genest also helped with the x-ray and ultrasonic imaging of the composites.

Like in the last paper, Dr Paquet helped with mentoring, planning of experiments, structuring of data, general advice on the project, and helping coordinate and follow up with the team to make sure everything stayed on track.

3.3 Abstract:

Monitoring the structural health of composites during manufacture and in-service is desirable to alert against damage or deterioration of conditions beyond an acceptable level. Wireless sensors embedded into materials that can endure the forming and curing of carbon fiber-reinforced polymer laminates will open the door to automated near-field detection of key metrics such as temperature, strain, and manufacturing defects. Current sensing technologies are generally too intrusive and fragile to be reliably embedded into laminates or too expensive to be applied commercially. The development of embedded, low-weight, small-footprint sensors is reported here, along with their use for monitoring stress and damage of a composite material matrix. These sensors consist of screen-printed discs, excited externally with an AC magnetic field to generate a secondary field, which have a temporary reduction in return signal when under stress, and a permanent loss of return signal after damage. This proof-of-concept work demonstrates how printed sensors can be fabricated to generate a high electromagnetic response, while minimizing their footprint in the laminate. Three sensor designs were evaluated as well as increasing the thickness of the silver by overprinting multiple layers. The substrate thickness and encapsulation scheme for the sensors were also tested to identify the sensor architecture that can detect matrix strain and damage. It was found that a three-layer screen printed disc directly in contact with the composite, printed on 1 mil Kapton had a relative signal loss of 10.6% after matrix damage, and an identical disc printed on 0.127mm Kapton had the same signal loss when the material was under stress of over 300N, but no signal loss after the damage. This work offers simplified sensor designs

with higher signal return the previous benchmarks as well as a strategy for designing and fabricating sensors capable of detecting matrix strain or damage by tuning the properties of the Kapton substrate.

3.4 Introduction

Carbon fiber reinforced polymers (CFRP) are widely used as structural materials in aerospace, automotive, and naval sectors, to reduce vehicle weight and fuel consumption (along with being corrosion free), due to their superior specific strength and stiffness properties. Generally, these parts are made by depositing carbon fiber pre-impregnated in a thermosetting matrix (prepreg) ply over shaped tools, and curing them in autoclaves. Most commonly, this is done manually by sequentially laying up full-field plies – a tedious and labor-intensive set of procedures. Conversely, there are a number of automated technologies, where narrow prepreg ribbons are sequentially deposited onto the tool. Their applicability is often limited by part complexities, inherit high costs, and low adaptability. Alternatively, forming technologies offer a compromise, where a flat laminate is assembled (either manually or using low-cost robotics), and then formed over the tool, simplifying and accelerating the process. All these processes carry a risk of various difficult-to-detect deposition defects, generally due to: operator mistakes, robot/part interaction errors, and formed ply waviness, respectively[1].

Non-intrusive, embedded sensors offering an insight into ply positioning would have potential to reveal processing defects, allowing non-destructive verification of the laminate condition mid-process, and thus enable information for rapid process modifications. Later on, they can be used for in-service health monitoring of the composite, alerting to the presence of matrix micro-cracks, delamination, and other critical defects.[2]–[11] They can also be used to monitor vibrations[12] or strains in material, statically or dynamically.[4][13]–[17] Furthermore, the

sensors proposed in this and previous publications work passively, and only require the energy remotely provided by the Eddy current testing to provide a return signal.[18]

Current embedded sensor technologies for monitoring the health of CFRP and similar composites face challenges with durability and sensitivity to temperature variations during manufacturing and throughout service life.

For example, piezoelectric material-based sensors can become depolarized at the high temperatures encountered during CFRP manufacturing, often exhibit poor homogeneity during production, and are prone to failure under the stresses and environmental conditions typical of aerospace applications.[3][8][12][19].

Another case would be fiber optic Bragg grating (FBG) sensors, which are costly, complex to develop, and require additional hardware. Their performance can be affected by temperature fluctuations, and they present difficulties in maintenance.[13][20][21]. Similarly, Brillouin optical time domain analysis (BOTDA), which requires specialized interrogation equipment and relatively long sensing times, make real-time monitoring challenging. Although BOTDA enables distributed strain measurement, its spatial resolution is limited compared to FBG sensors, and the accuracy can degrade in areas with sharp strain gradients. In addition, installation and calibration can be complex, and the overall cost and hardware requirements increase its difficulty of implementation and long-term upkeep[22].

Fiber optic acoustic emission sensing is another approach for composites, as damage-induced stress redistributions in a structure generate high-frequency pressure waves. However, the signals are very low in amplitude and strongly attenuated in composite materials. Furthermore, damage mechanisms in carbon fiber such as fiber breakage, matrix cracking, and interfacial fretting, produce more complex and less understood acoustic signatures[23].

Other technologies also exist such as using thermochromic paint, which provides a more sensitive means of detecting damage cause by thermal stress. The paint works by transitioning from a non-fluorescent to a fluorescent state when exposed to harmful time–temperature conditions, enabling wide-area visual inspection using a removable polymer film. However, this comes with the limitations of more difficult application and possible incompatibility with composite coatings, and more subjective results.[24]

Therein lies the novelty of the presented research, which combines the superior insight of fiber optic-based solutions without the need for fiber optics and its inherent disadvantages, and the simplicity of printed electronics, but most importantly it does so with no performance or structural integrity penalty to the composite material.

To better monitor the state of CFRP structures, a monitoring system of embedded coil sensors was proposed in previous work[18], which had the following requirements: the ability to accurately indicate ply position (from which ply migration can be inferred), not be invasive (i.e. not affect ply behavior, be compatible with the forming process, and be small enough to not be considered an inclusion), able to provide continuous measurements, be durable (survive forming, curing, and other post-processes), and able to provide qualitative and quantitative data.

Our previous work focused on identifying a method of monitoring ply migration using eddy current methods. However, the approach we developed however was limited to measuring ply migration only, which helped identify issues during manufacturing, but it did not provide updates about the health of the composite throughout its service life. Additionally, the fact that the sensors were complex to manufacture, requiring careful intervention to connect the terminals of the sensor, in addition to post manufacturing treatments in the form of copper plating to further increase sensitivity.

A new generation of sensors is proposed in this paper with the goal of simplifying the manufacturing process, as well as increasing their performance to be able to report on the health of a composite throughout its service life, whilst still meeting its previous requirements. This new generation retains screen printing as its main manufacturing method, which remains an attractive solution as they can be wirelessly read with reflection type eddy current probes, are inexpensive to manufacture, and fall below the threshold size of an inclusion. In addition, this new generation explores new shapes such as concentric rings and discs; new architectures, such as multi-layer printing of a sensor, allowing for a significant increase in signal with minimal impact to sensor dimensions. Furthermore, the sensors are directly in contact with the composite matrix), allowing the sensor to respond to matrix damage or strain, reducing the signal return of the sensor that can be used to alert for changes in material health.

Similarly to our previous work, eddy current methods, an industry standard technology for non-destructive testing, are used to monitor the composite. The technique is based on electromagnetic induction and can detect small defects in metals and do not require intimate contact with the part under investigation [25]–[27]. Utilizing this technique to detect embedded sensors in composites leverages its broad industry usage, thereby reducing the need for additional testing equipment and extensive training. This technology allows the periodical measurement of the electromagnetic response of the sensor embedded within the composite material throughout its service life to monitor its structural health.

The goal of this work is two-fold: first, to identify screen printed sensors that are simpler to manufacture but also produce stronger signal, and second, to design the sensor such that it can detect changes to the matrix. The method uses screen printed molecular silver inks that have high

printing resolution and low film thickness ensuring the sensors maintain a small footprint within the laminate[18].

Like in previous work, these sensors must survive the harsh conditions of the forming and curing steps, as well as have a minimal physical area to ensure negligible impact to the laminate behavior and integrity. This work first reports on the different performance of various sensor shapes, such as concentric rings, discs, and multilevel prints, comparing them to the previous generation of sensors, which are used as a baseline. Thereafter, we compare the impact of different sensor architectures and the way they interface with the composite, showing how their signal return changes when the matrix is under strain, and can be permanently lost when sensors themselves suffer damage.

The approach to sensing has been further optimized and offers the opportunity to streamline the sensors and increase performance. The proposed work here is unique, as it puts forward a new approach to non-contact and in-situ monitoring of CFRP manufacturing, and it paves the way for printed embedded sensors in structural health monitoring using convenient non-destructive techniques.

3.5 Experimental

3.5.1 Screen Printing

Meshtech NBC [28]fabricated the screen with the desired sensor pattern using photoimaged MM1 emulsion (10−14 μm) supported on a SS360 stainless steel mesh. The methods to prepare and print silver molecular inks are described elsewhere[29]. The ink is based on silver neodecanoate combined with a polymeric binder, and with a final viscosity of 5000-6000 cP. A polyimide film, Kapton, was chosen as a substrate for its compatibility with the processing conditions used in forming the CFRP, most importantly its chemical and thermal stability. Sensors

were prepared by screen printing the molecular ink onto 21.6 cm × 27.9 cm sheets of polyimide film using a flatbed American M&M S-912M [30]small format screen printer.

3.5.2 Post-Printing Processing

The silver prints were processed following the methods from Liu et al and Wagner et al.[31][32] which consist of UV curing followed by thermal sintering. To connect both terminals of the spiral sensors, small perforations were made through the polyimide film, a thin and narrow silver ink trace was deposited with a syringe on the back of the substrate to complete the closed-loop spiral. Then the curing and sintering process was repeated to make the back-trace conductive. For multi layered sensors, each layer was UV cured, then printed on again depending on the amount of layers required, and lastly thermally sintered.

3.5.3 Composite Manufacturing

The sensors underwent forming and curing processes. First, the sensors were fully encapsulated in 0.0254 mm thick polyimide tape coated in pressure-sensitive silicone-based adhesive. Then, they were embedded during the hand layup deposition of the prepreg plies for the manufacture of a flat preform, using a typical aerospace unidirectional carbon / epoxy composite prepreg. Each laminate was sized (304 mm × 76 mm × 1.35 mm) for 3-point bend mechanical testing. Also, the laminate cross-ply design [90/90/0/90/0]S was selected to favour matrix loading during bending, ensuring its cracking under low mechanical load. The expectation that the sensor printed layers would experience similar behaviour and thus report a change in observed signal. Furthermore, various sensor print methodologies and encapsulations would result in different signal response under similar loading conditions.

Each laminate was equipped with two sensors centrally placed between the most vulnerable plies 9 and 10, and separated by 25.4 mm. The laminates were placed between flat tool and caul

plates to ensure flatness, and cured in an autoclave, at 6 bar, 177°C for 5 hours. Using the eddy current procedure described below, the sensors were interrogated before the encapsulation, after the preform assembly, curing, laminate trimming, and during the mechanical testing. The data was then processed with VBA and MATLAB scripts. No change in signals was detected due to the encapsulation, and trimming. As expected, both preform assembly and cure consolidation resulted in change of stand-off between the sensor and the detector. These were accepted as new signal baselines.

3.5.4 Mechanical testing

Each laminate was subjected to various bending stresses, while monitoring the sensors response and listening for matrix cracking. The external sensing copper coils (7 turns, 300 μm wide traces, 17.5 μm thickness, printed on flexible substrate) were adhered to each coupon on the embedded sensor side, thus maintaining the sensor to coil distance during the test. Eddy current interrogation of the sensor return signal of the were taken directly on the load frame by connecting a Tektronix 2 Series MSO24 oscilloscope and a Tektronix Function Generator AFG3102 set to 20 MHz and 10 Vpp to a current-limiting resistance in series with the interrogating coils and the ability to interrogate either of the two coils.

The test protocol was to install the coupon in a 3-point bend fixture, affixed to a hydraulic MTS - 3.5 Kip Capacity Test Frame. After establishing a zero-load baseline, the load was increased by 30 N until 300 N were reached, while taking a measurement at every step. The load was released, and the loading pattern was repeated. At the end of the third cycle, the coupons would have been further loaded by steps of 30 N until cracking was heard. The load was released and final sensor condition evaluated. Laminates 2 and 4 had their load increased until visible damage

to the coupon, which was considered matrix failure. The error shown in the figures is that of the equipment, since the sensors in each coupon were measured individually.

3.5.5 Characterization

The sensors were characterized using several techniques. A CT100 Cyber Technologies optical profilometer was used to measure height, thickness, and surface roughness of the printed sensors. Eddy current testing was done to validate performance in the green and cured states of the composite. This was done using an EC TecView Acquisition and Analysis software and hardware, with a transmit-receive reflection type EC probe consisting of an outer excitation coil and an inner receiver. The frequency tunning of our three-coil (inductor, sensor, and receiver) system was determined experimentally, and found to be in the range of 100-250 kHz; subsequently, we used a frequency of 200 kHz to drive the transmitter component of our eddy current probe. The probe was excited with a 200 kHz, 10 Vpp sinusoidal waveform, while a 40 dB gain was applied to the receiver signal. The scanning probe was mounted on a robotic arm to enable scanning a planar (horizontal) test piece at a speed of 12mm/s, and a step of 1mm on both scanning and indexing directions. The measurements were taken at separations (on the vertical axis) varying from 0 mm up to 4 mm between the sensor's plane and the probe. In addition to the excitation coil, the scanning probe contains an inner, concentric coil, shielded from the excitation one which allows for the reading of the signal from the sensor. The voltage amplitude of the receiving coil is the feature used for analysis. This amplitude is expressed as a percentage, as based on the recorded orthogonal eddy current signal components, with 100% representing the maximum on a scale of 5 Vpp, after application of the gain settings. The ultrasonic scanning was conducted with a TecScan immersion system through transmission at a frequency of 10 MHz. A focused probed with a Probe Type: Focused probe with a 3.0" focus and scan increment steps 0.5 mm were used to perform the scan.

Lastly, x-ray imaging was performed with a Lorad 160 inspection system: on laminates L1 and L2 the tube voltage was 60 kV, a tube current of 4 mA, and an exposure time of 12 seconds; on laminates L3 and L4, the tube voltage was 80 kV, tube current was 4 mA, and exposure time was 12 seconds.

3.5.6 Naming convention of samples

The naming convention for the embedded sensors is comprised of three elements: a number indicating the number of printed layers in a sensor ranging from 1-3; a letter which indicates if the sensor is directly touching the composite, T for sensors directly in contact with the composite, or K for sensors encapsulated in polyimide, and not directly in contact with the composite; and lastly, another letter which specifies the thickness of the polyimide substrate used, which can be T for 1 mil polyimide and R for 5 mil polyimide. ESI 1 illustrates the differences between each type of sensor.

Four laminates with different embedded sensors were tested : Laminate 1 (L1) had 1KT and 2KT, Laminate 2 (L2) had 3KT and 3KR, Laminate 3 (L3) had 1TT, and 2TT, and Laminate 4 (L4) had 3TT and 3TR.

3.6 Results and Discussion

In our previous work, CFRP-embedded planar spiral coils, when excited and sensed via electromagnetic induction with a transmit–receive eddy current probe scanning the composite part were effective sensors for monitoring ply migration during forming and curing parts. However, these sensor designs proved difficult to manufacture consistently, due to the need to physically connect the front and back sides of the sensors to create a closed loop circuit. This step required extensive manual intervention for each coil fabricated and therefore negated the advantage of using screen printing, which can manufacture a large amount of identical sensors with little extra effort. In this work, simpler sensor designs that do not require the manual intervention, as shown in Figure 1a, were evaluated

These new architectures include the original planar single sided spiral coil (which still manual required intervention), to be used as benchmark; concentric rings, and discs, which would provide the most signal return, though they would probably retain the most performance when damaged. Each sensor design was fabricated with diameters ranging from 3.9mm to 10 mm.

Figure 1b shows the performance of each sensor at a standoff distance of 0 mm and gain of 40 dB gain from the EC probe. It can be seen that discs have the strongest signal return out of the 3 designs. For instance, the discs of 10 mm had a signal return more than 2 times that of the spirals, and more than3 times that of the concentric rings. Furthermore, discs with a diameter 25% smaller (7.5mm) than their spiral and ring counterparts (10.1mm) had signal return within each other's standard deviation, meaning their performance was statistically similar despite their smaller size. Lastly, spiral and concentric ring sensors performed similarly, with signal returns within each other's standard deviation for sensors with diameter less than 9 mm.

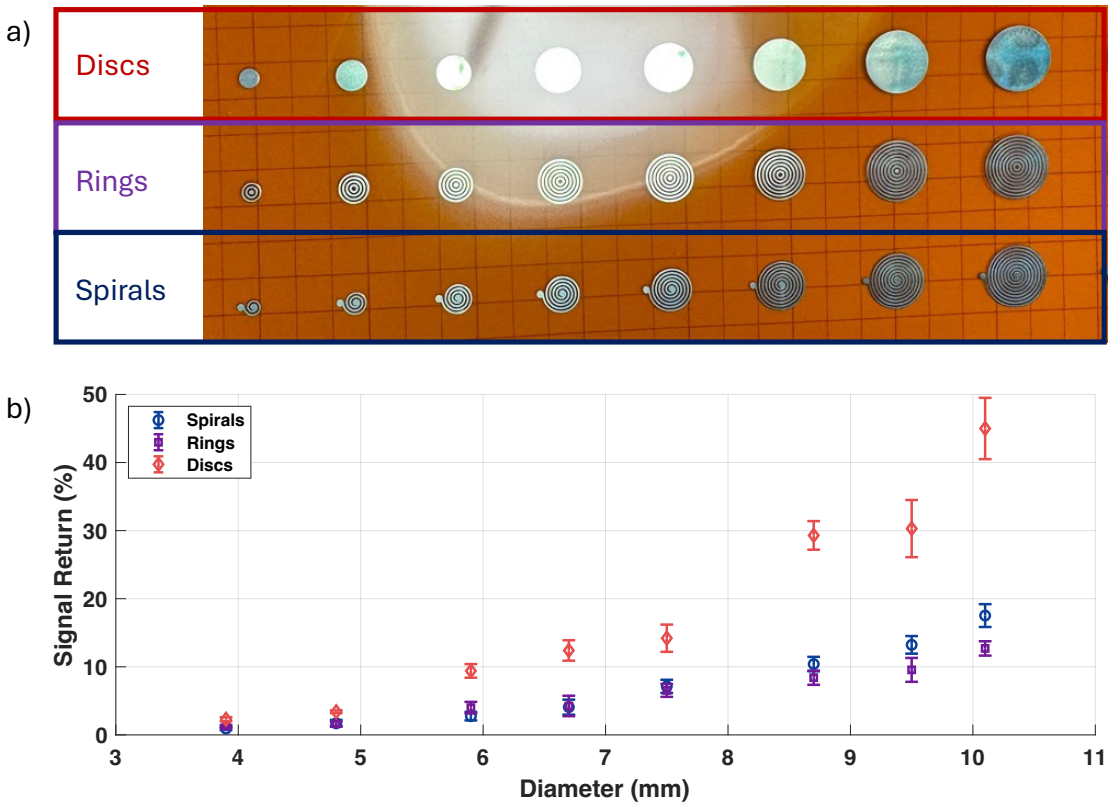

***Figure 12**: a) Disc, Ring, and Spiral sensors of 8 sizes, ranging from 3.9mm to 10.1mm b)Performance comparison of disc, ring, and spiral sensors.*

These results indicate that the volume of conductive silver that make up the sensor has a strong correlation to sensor sensitivity, more so than the shape of the sensor. To test this theory, disc sensors that were overprinted to make single, double, and triple layer sensors were manufactured, scanned with an optical profilometer, and measured with an EC probe..

Figure 2a shows the topographical scans for the three different disc sensors manufactured. It was found that each layer added 0.8 um in thickness but also increased the variability in thickness; the single layer sensors measured 0.82±0.03 um, the double layer sensors measured 1.82±0.31um, and the triple layer sensor measuring 2.70±0.48 um.

Figure 2b shows an EC scan of single, double and triple layered sensors, and Figure 2c shows their signal return at 0 mm standoff and 0 dB gain. The gain was reduced to 0 dB for these

measurements to allow for a better understanding of sensor performance, since a gain of 40 dB was causing the signal to saturate.

It can be observed that the sensor thickness has a proportional impact on the return signal, with the double and triple thickness sensors returning double and triple the signal respectively for most sensor sized. Effectively, this means that an 8.7mm three-layer disc, has a 3 times stronger signal than a single layer one, which also has a signal 3 times stronger than a spiral / ring of an equivalent size.

Two important advantages result from these new sensor designs in comparison to our previous work[18]. First, a 3x improvement in return signal compared to the highest performing previous design, that is achieved by using triple-layer disk shape. This is significant as it affords greater freedom in how the sensors can be used. In our previous work, the sensors signal output was sufficient to read through a composite material 4 mm in thickness. With a 3x improvement in return signal, sensors can be embedded deeper within a composite, or sensors with a smaller diameter can replace previous generation sensors of a larger diameter. A more sensitive sensor positioned deeper in the composite allows for identifying manufacturing defects in composites with more layers, and a smaller sensor allows for even less impact in the composite performance both in weight and mechanical properties. Secondly, the fabrication process of these sensors is significantly simplified as it does not require the manual step of electrically connecting the spirals printed on both faces of the substrate while also eliminates the copper plating step.

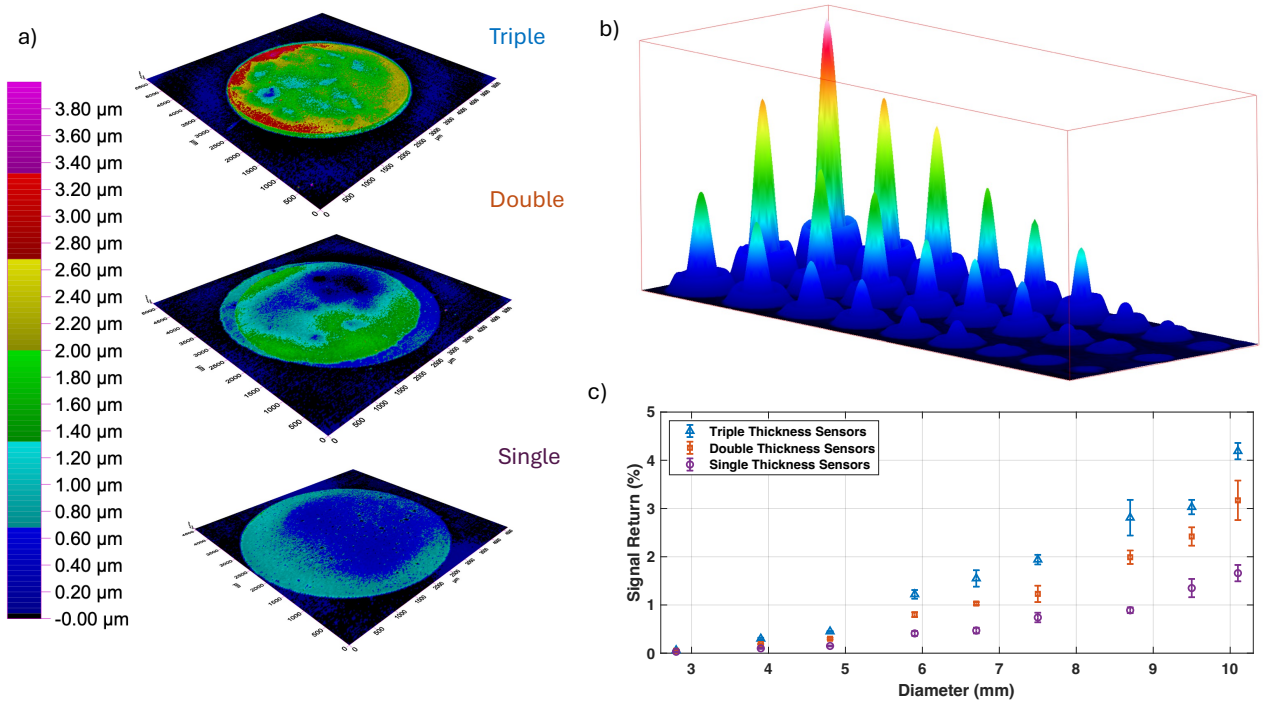

***Figure 13**: a) Optical profilometry scan of single, double, and triple thickness disc sensors b) EC scan of the three different types of sensors: Single layered sensors on the left, double layered sensors in the middle, triple layered sensors on the right. c) Signal return comparison of single, double, and triple thickness discs.*

In the first iteration of this work[18], the sensors were used to track the movement of plies during the forming and curing steps. In this work, we build on these advances to expand the functionality of the sensors to detect structural damage and monitor strain while the CFRP specimens are subject to load. The response of the sensor when the matrix is strained or damaged will depend on the architecture and properties of the sensors. To identify the role of sensor encapsulation and sensor thickness on its response to matrix stress, several series of sensors were fabricated, each using discs with an 8.7mm diameter. More information on the exact varieties, nomenclature, and diagrams is available in the experimental section. The first series used for the initial load case study, shown in Figure 3, consisted of discs with directly in contact with the

composite (not encapsulated) printed with a single, double and triple layer of silver ink and are referred to as TT1, TT2 and TT3, respectively. The second series also consisted of a single, double and triple layer of silver ink but were encapsulated with a top layer of 0.0254mm polyimide, and are referred to as KT1, KT2, KT3, respectively. Both series were printed on 0.0254mm polyimide substrate. Schematics of these two series are found in Figure 3a and 3b. The TT series was used to evaluate whether the surface of the sensor would bond to the composite matrix, allowing stress to propagate from matrix to sensors, causing damage to the sensors that would be detected as a change in return signal. The KT series was used as a control to validate whether the stress-induced matrix damage reduce the sensor performance or the stress induced damage on the sensor itself.

Figure 3c and 3d only show the initial stressing of the composite pieces, from 0N to 300N, with steps of 30N, which is where each measurement was taken. Figure 3c shows that with the exception of the single layer discs, the return signals of the sensors progressively decreased as the applied load was brought up to 300N. At a load of 300 N, cracking of the composite was heard in concert with the measured drop in signal for the sensors was observed. Such was the case for double and triple layer sensors, which had a statistically significant drop in signal strength when compared to the initial reading.

At the end of the this first cycle when load was returned to 0N, all 3 sets of sensors returned to their original value of signal return, showing that they could also measure the strain in the composite matrix though only at higher stresses. Subsequent stress cycles will be explored in latter case studies.

Figure 3d shows, contrastingly, that single and double sensors which were completely encapsulated in polyimide presented negligible change in signal when stressed to 300N, whereas their half-encapsulated counterparts presented 2.4% change for the single layered sensor, and

almost drop 8.8% for the double layered one. The triple layer sensor only showed a drop of 2.4% at 270N, half of that of the half encapsulated one at 4.8%. This case study showed that some strain can be measured with the sensor that are directly in contact with the composite, and that the thicker sensors also present a higher drop in signal under stress. However, it is important to note that a small percentage of that change in signal is due to the sensor itself stressing.

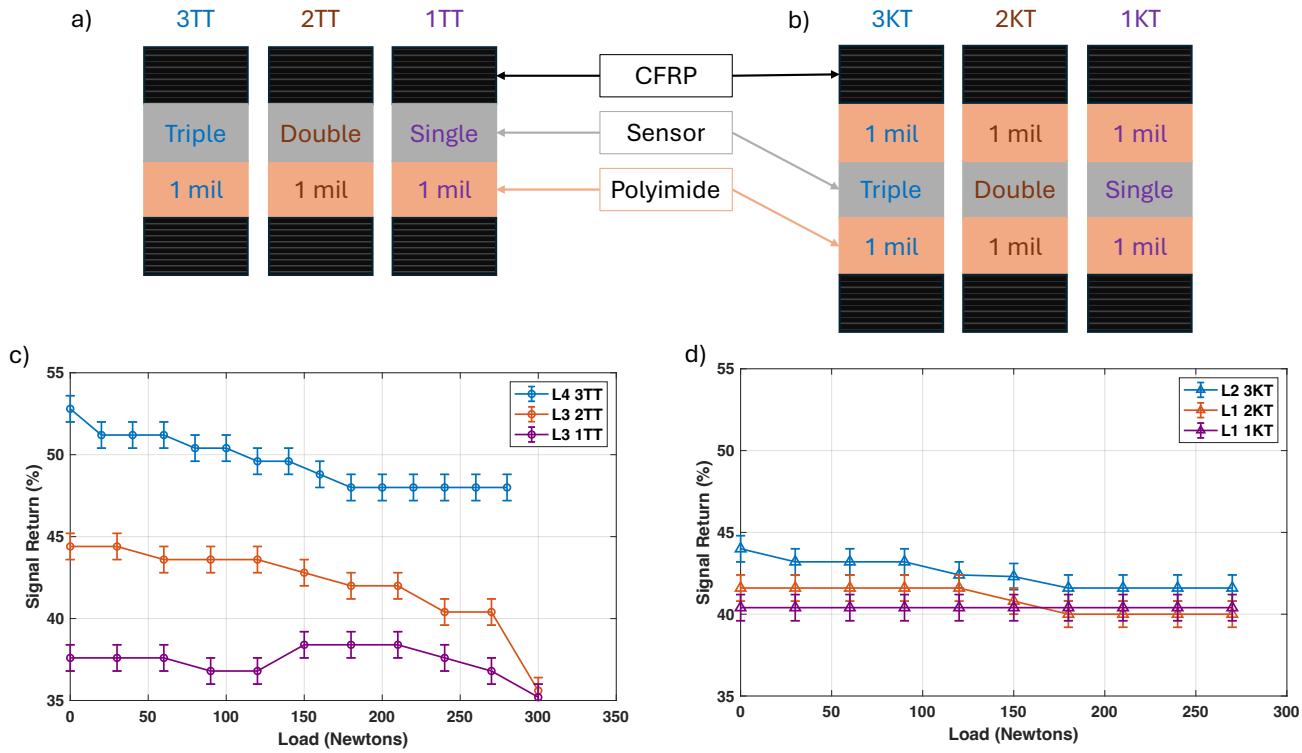

***Figure 14**: a) architectures of non-encapsulated single (1TT), double (2TT), and triple thickness (3TT) sensors printed on 1 mil polyimide. b) architectures of encapsulated single (1KT), double (2KT), and triple thickness (3KT)sensors printed on 1 mil polyimide. c) Signal return of non-encapsulated sensors on their first stress cycle from 0-300N d) Signal return of encapsulated sensors on their first stress cycle from 0-300N*

Whilst the strain in a composite is an interesting aspect to be able to measure, current advancements in this technology still limit its sensitivity, and therefore usability, in wider applications. A real change in signal only starts showing when the sensor is close to matrix damage. Matrix damage measurement is a much more promising and reliable datapoint that can be obtained with the sensors in their current state.

Figure 4a and 4b show an ultrasonic and x-ray scan of a composite with 2 sensors embedded, which directly in contact with the composite. The X-ray image indicates limited visible damage. However, subsequent ultrasonic inspection reveals significant matrix degradation, as indicated by the red regions in the scan. In this imaging scale, red corresponds to reduced signal return, whereas green represents areas with intact matrix and strong signal reflection. This damage can be observed mostly in the middle of the cutout, where the 3-point bend test was conducted. Only data of the 1st full cycle and the 3rd cycle after 300N (to improve readability) is plotted in figures 4c and 4d, further details of the stress testing are explained in the experimental section. The composite was heard cracking where the red circles are plotted in each figure, starting at 300N. These figures show that after sustaining matrix damage, the signal return of the sensor was permanently reduced for both single- and double-layer discs. It can also be observed that the signal loss for the 2-layer sensor was twice that of the single layer one. From this we concluded that the thicker sensors are more susceptible show a change in signal from damage caused by stressing the composite.

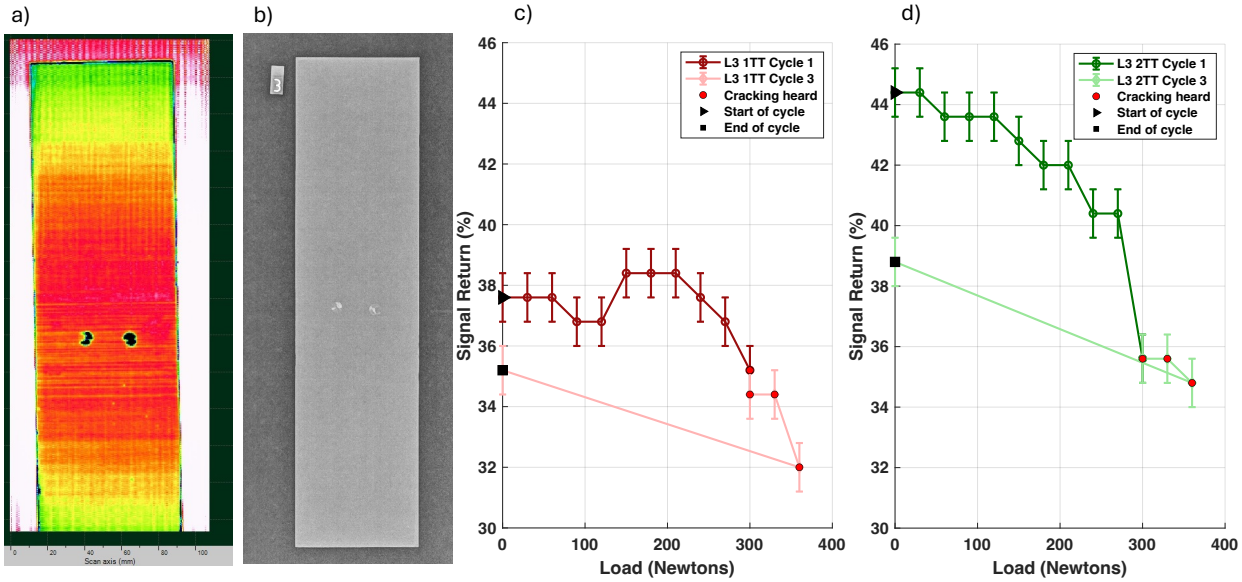

***Figure 15**: a) Ultrasonic scan of laminate 3 (L3), which had one single layer non-encapsulated (1TT) sensor, and one double layer (2TT) non-encapsulated sensor. b)X-Ray scan of laminate 3 (L3), which had one single layer non-encapsulated (1TT) sensor, and one double layer (2TT) non-encapsulated sensor. c)Signal return of non-encapsulated single layer (1TT) sensor on its first and last stress cycle, with red dots indicating when cracking was heard. d)Signal return of non-encapsulated double layer (2TT) sensor on its first and last stress cycle, with red dots indicating when cracking was heard.*

The next step was to validate the possibility of strain permanently reducing sensor signal due to material properties of the sensor. As to rule out the possibility of the sensor being damaged by straining on its own, therefore not measuring the damage to the matrix but the damage to itself. To do this, coupons L2 and L4 were put under stress as described in the experimental section. Composite L2 had a fully encapsulated three-printed-layer sensor (3KT) embedded; and composite (L4), with a three-printed-layer sensor directly in contact with the composite; only composite L2

was stressed to the point of failure which happened at 330N. On the other hand, composite 4 was put under a maximum load of 380N, when heavy cracking was heard and the testing was stopped.

An x-ray of the composite piece L2, with the failure point clearly visible in the middle can be seen in Figure 5a, and one of composite L4 can be seen in figure 5b. Triple layer sensors were used for this case study, since they were the most sensitive to signal change under strain, so of any signal was to be lost, a triple layer sensor would be the most sensitive to it. Figure 5c shows the sensor in contact with the composite in blue, and the fully encapsulated one in orange. Out of the three stress cycles run, only the first and the last are plotted for clarity. It can be observed that the sensor that was directly in contact with the composite had permanent loss of 4.8% in signal at the end of its last stress cycle, with temporary reductions when under stress. In contrast, the fully encapsulated sensor had no statistically significant signal drop, even after complete failure, it also had very little signal change under straining.

From this case study we can conclude that the permanent signal drop that can be observed after some damage to the matrix occurs, is in fact measuring damage to the matrix, and not to the sensor itself.

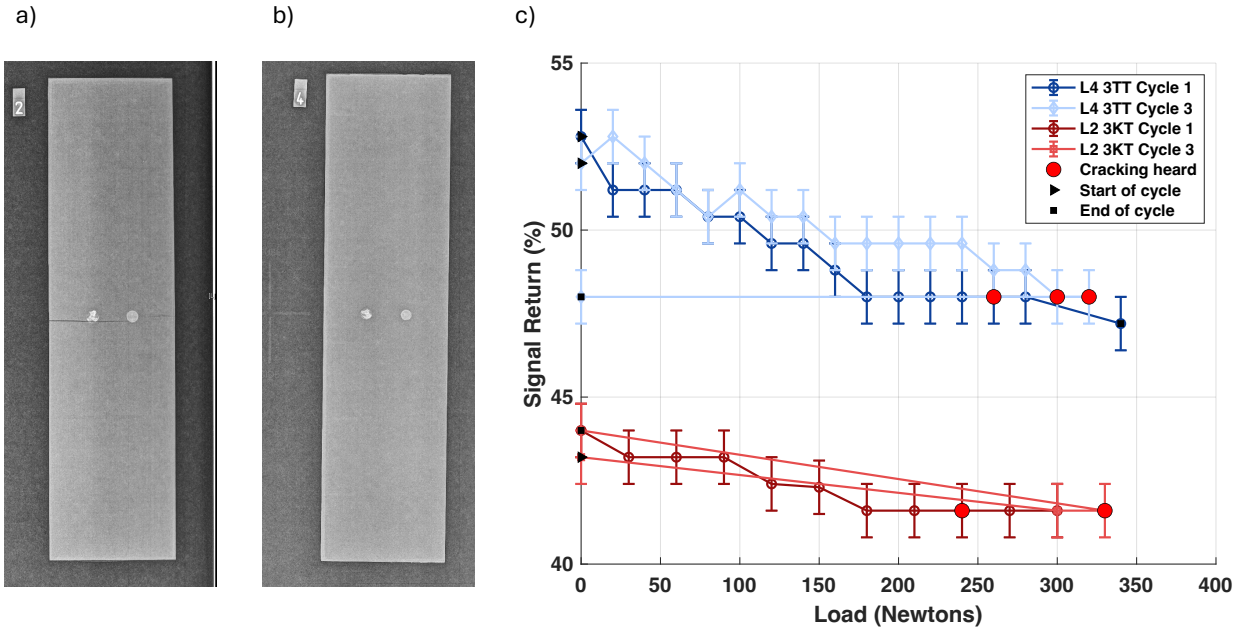

***Figure 16**: a) X-Ray scan of laminate 2 (L2), which had one triple layer encapsulated (3KT) sensor, and one triple layer printed on 5 mil polyimide (3KR) encapsulated sensor. b) X-Ray scan of laminate 4 (L4), which had one triple layer non-encapsulated (3TR) sensor, and one triple layer printed on 5 mil polyimide (3TT) non-encapsulated sensor. c) Signal return of non-encapsulated triple layer (3TT) and encapsulated triple layer sensors on its first and last stress cycles, with red dots indicating when cracking was heard.*

As a last case study, the impact of the substrate on the sensor performance was studied. Identical triple-layer sensors were embedded, both directly in contact with the composite. The only difference was that one of them was manufactured with 0.127mm polyimide film as substrate, and the other with 0.0254mm polyimide film, a diagram of these can be found in figure 6a.

The main finding from figure 6b is that whereas both sensors are equally sensitive to strain, which can be seen by their similar change of signal under load, which is a drop around 5% after 300N; only the sensor printed on thin 0.0254mm substrate was damaged by strain, as indicated by the lower return loss after removing the load. That is to say, the ability to measure damage was

greatly impacted by the substrate, with a thicker substrate of 0.127mm making it impossible to detect damage. This is presumably due to the fact that the thicker substrate offered more stability to the trace, therefore shielding it.

This finding further increases interest in pursuing manufacturing techniques where the substrate can be fully removed, which should result in even more accurate damage and stress measurement

Figure 6c shows significant damage on the composite piece itself. The loss of signal return from the ultrasonic scanner can be interpreted with the different colors, which go from green (where the return shows no damage) and change to red, where there is a significant loss in signal due delamination and matrix damage, and finally black spots which show strong reflection (ie the embedded sensors) or complete signal loss due to cracks and structural failure of the composite. This corroborates the finding that sensors printed on a thinner substrate measured the damage to the composite instead of damage to the sensor itself.

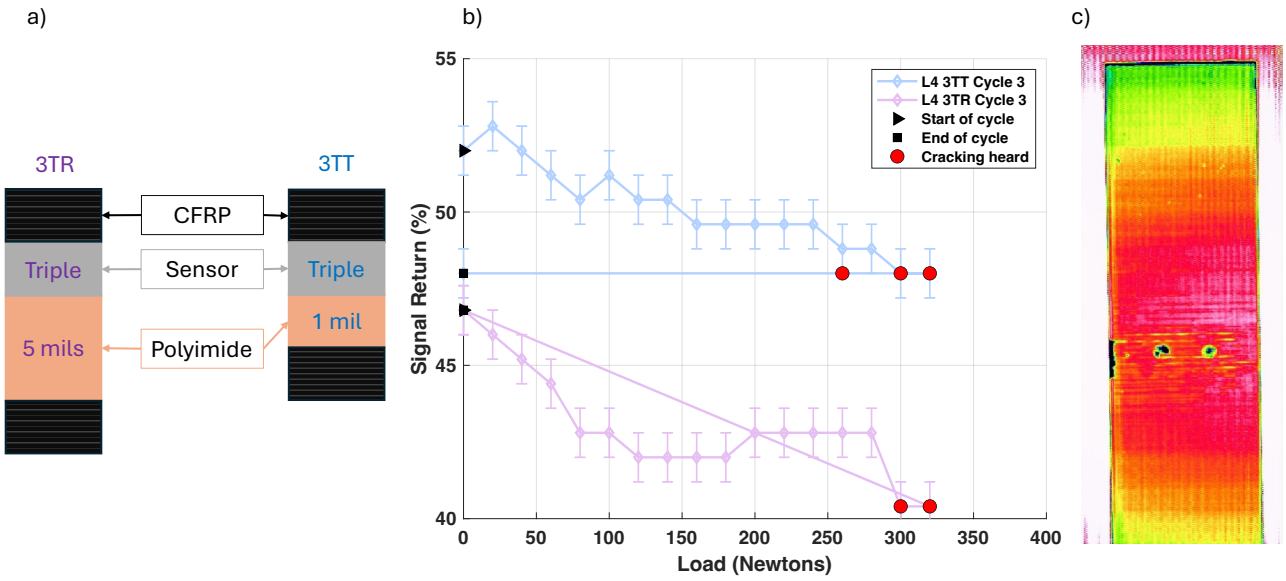

***Figure 17**: a) architectures of non-encapsulated triple thickness sensors printed on 1 mil polyimide (3TT) and 5 mil polyimide (3TR). b) Signal return of non-encapsulated triple thickness sensors*

printed on 1 mil polyimide (3TT) and 5 mil polyimide (3TR) on their first and last stress cycles, with red dots indicating when cracking was heard. c) Ultrasonic scan of laminate 4 (L4), which had one non-encapsulated triple thickness sensors printed on 1 mil polyimide (3TT) and one non-encapsulated triple layered sensor printed on 5 mil polyimide (3TR).

3.7 Conclusion

This proof-of-concept study investigated the use of a novel passive electromagnetic sensor to monitor damage and strain of a composite material (CFRP). The sensors were manufactured via the inexpensive and scalable method of multi-layer screen printing. The printed conductive discs, rings, and coils, generate a magnetic field when externally excited, allowing for near-field sensing. Various shapes and architectures were evaluated and led to the identification of a sensor platform that has a small footprint, high durability, and performance, as well as good survivability to high temperatures and low pressure used during curing and forming of CFRP. It was demonstrated that triple layered disc sensors had a signal three times larger than the previous generation best performing sensor (double sided, copper plated), twice that of coils, and three times that of concentric rings for the largest manufactured size od 10.1mm. Furthermore, it was found that concentric ring sensors have statistically similar performance to spiral sensors under 9mm diameters, whilst being much easier to manufacture.

The manufactured sensors provided valuable insight into strain and damage sensing in a composite. This was tested by embedding them into composite cutouts and measuring their signal changes during 3 cycles of 3-point bend tests up to a load 300N, and also until observable matrix damage.

Depending on the architecture of the sensor, we were able to individually measure for damage and strain to the matrix. The former was observed as a permanent drop in signal return of

4.8% after matrix damage for triple layer sensor that was directly in contact with the composite printed on 1mil polyimide as substrate. The latter was observed as a drop in signal of 6.4% when 300N were applied and a return to the original value when no longer under strain for a triple layered sensor printed on 0.127mm polyimide substrates.

We know the properties that were measured were directly related to the composite and not due to sensor material deformation, as additional sensors that were fully encapsulated in polyimide did not show a permanent change in return signal even after catastrophic failure of the composite. In fact, they only showed minimal signal loss when under strain. The damage to the composites was also evaluated with x-ray and ultrasonic imaging.

The embedded sensors proposed in this paper are an improvement upon previous work, which was only useful for measuring manufacturing defects and ply migration monitoring, now providing the ability to measure damage and strain to the composite matrix.

Future work will involve harnessing new technologies in order to embed the sensor directly into the composite, without the need for any polyimide films, as well as further increasing the sensitivity of the sensors to both damage and strain.

3.8 Supplementary Information

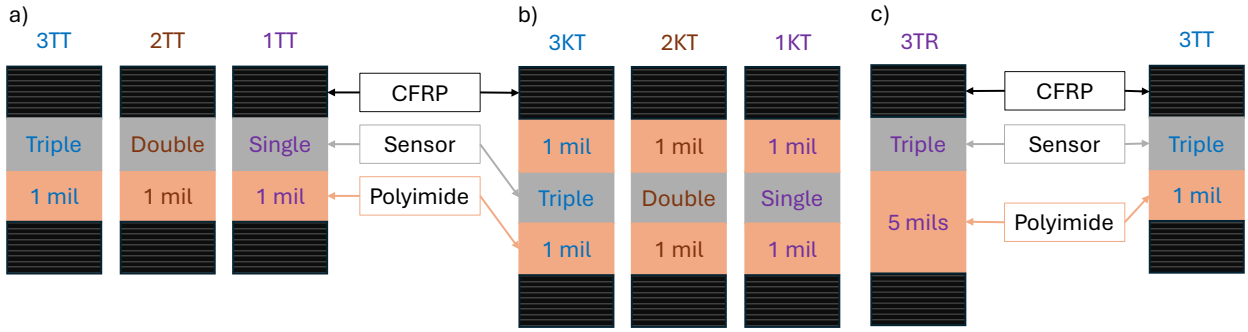

ESI 3.1: Strain and damage sensor architectures

a) Single, double-, and three-layer sensors directly in contact with the composite once embedded, printed on 1mil polyimide substrate

b) Single, double-, and three-layer sensors encapsulated in polyimide, not directly in contact with the composite once embedded, printed on 1mil polyimide substrate

c) Three-layer sensors directly in contact with the composite once embedded, printed on 1mil and 5 mil polyimide substrate

***ESI 3.2**: Spiral, Concentric ring, and disc sensors*

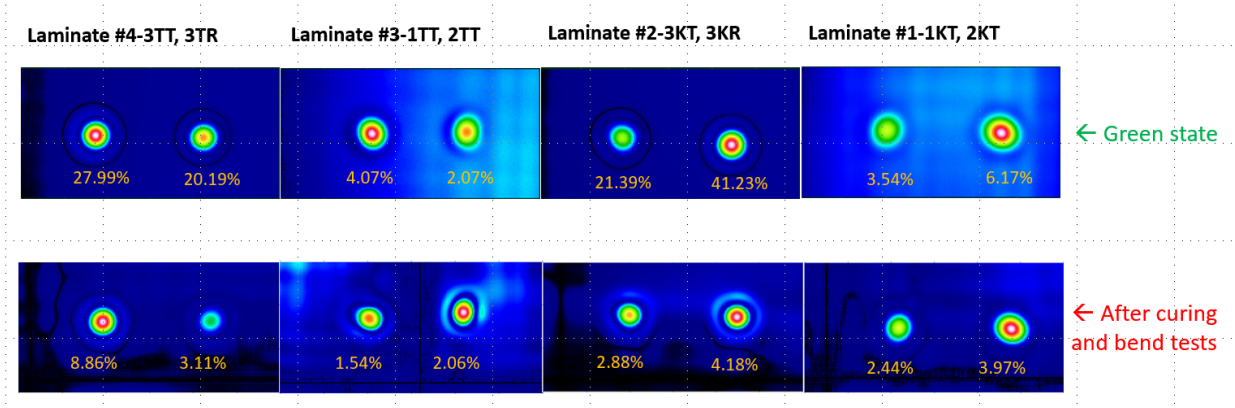

***ESI 3.3**: Laminates 1,2,3, and static EC Scan*

Sensor / Cycle	Initial	End of 1st Cycle	Start of 2nd Cycle	End of 2nd Cycle	Start of 3rd Cycle	End of 3rd Cycle	Final
1TT	37.6%	-2.4% (300N)	-0.8% (0N)	-4.0% (300N)	-0.8% (0N)	-5.6% (360N)	-2.4% (0N)
2TT	44.4%	-8.8% (300N)	-5.6% (0N)	-8.8% (300N)	-4.0% (0N)	-9.6% (360N)	-5.6% (0N)
3TT	52.8%	5.6% (340N*)	-4.8% (100N)	-5.6% (380N)	-0.8% (0N)	-4.8% (320N)	-4.8% (0N)

***ESI 3.4**: Table showing the change in signal readout from 1TT, 2TT, and 3TT sensors at different points of the stress test*

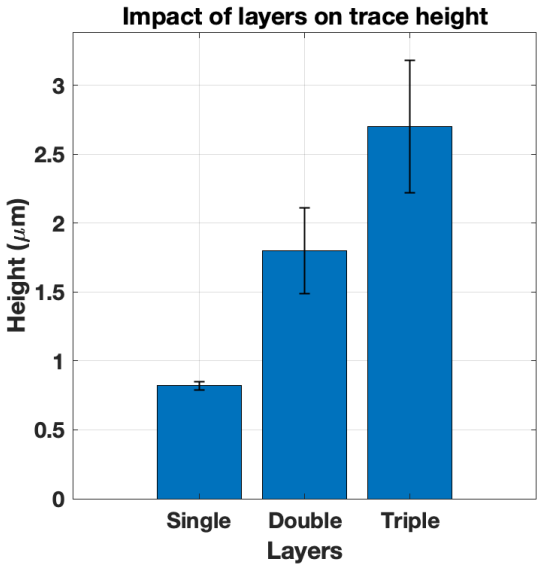

***ESI 3.5**: Figure showing the change in thickness of a sensor as a function of number of printed layers*

***ESI 3.6**: Initial setup of sensors for 3-point bend test, including the oscilloscope, switch, and function generator (Left). Laminate 4 before stress testing (Right).*

***ESI 3.7**: Laminate 2 during 3 point bend test (Left). Final setup for 3 point bend test (Right).*

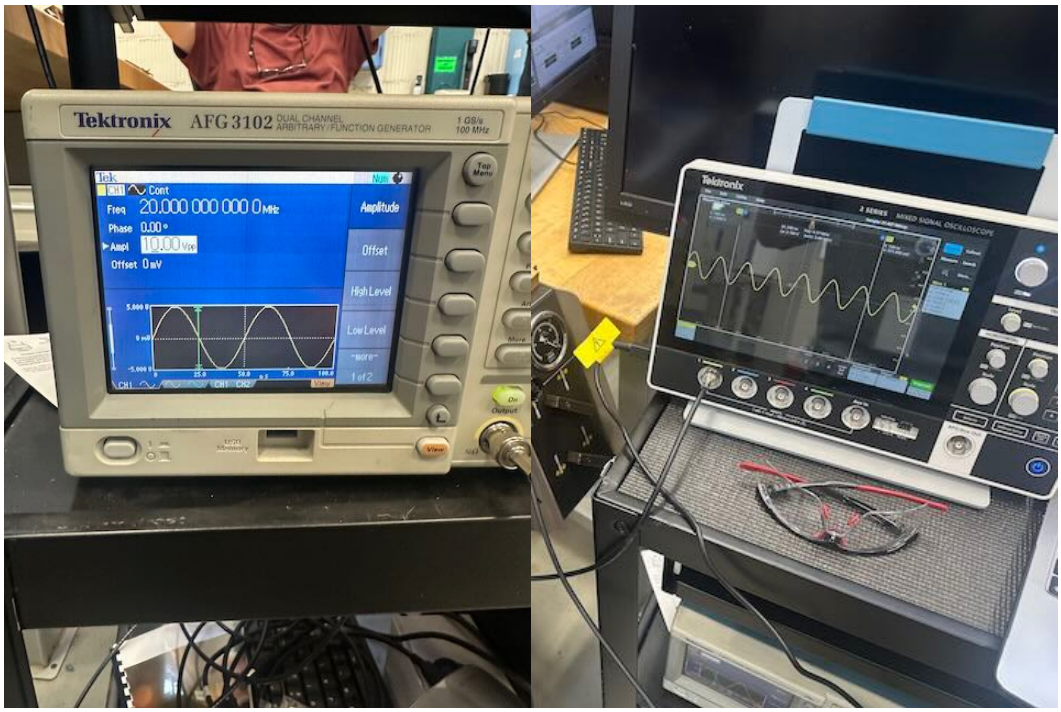

***ESI 3.8**: Picture of function generation during 3-point bend test (Left). Picture of oscilloscope during 3-point bend test (Right).*

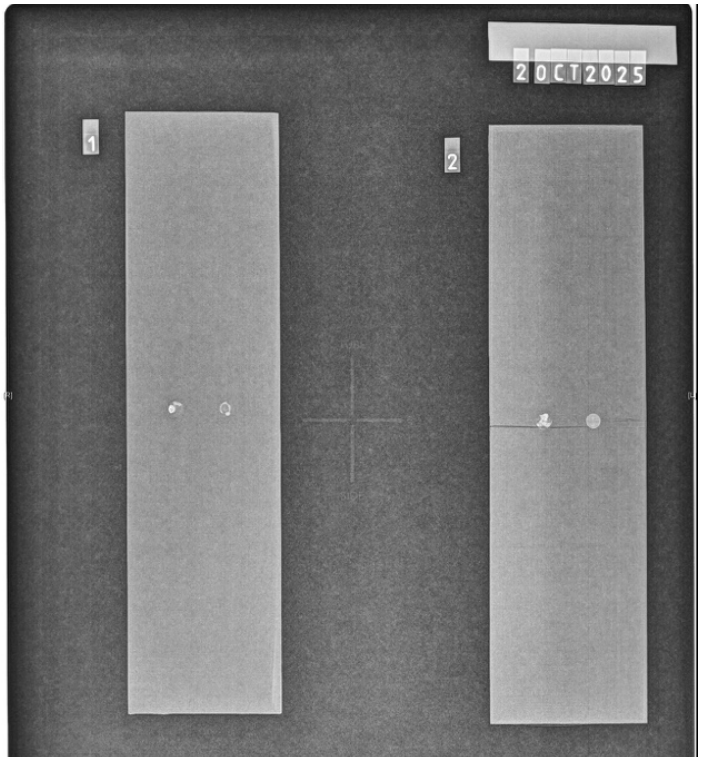

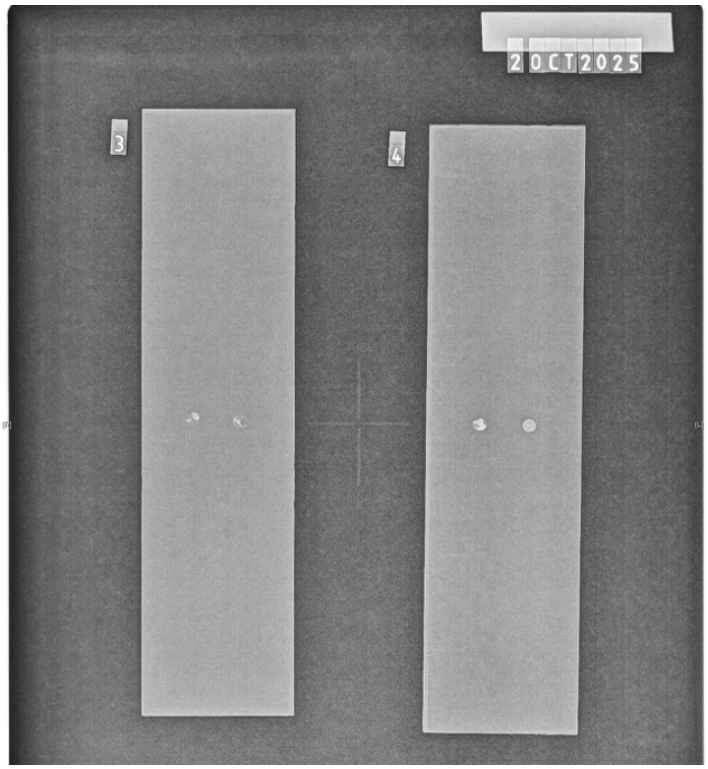

ESI 3.9*: X-ray images of laminates 1 through 4*.

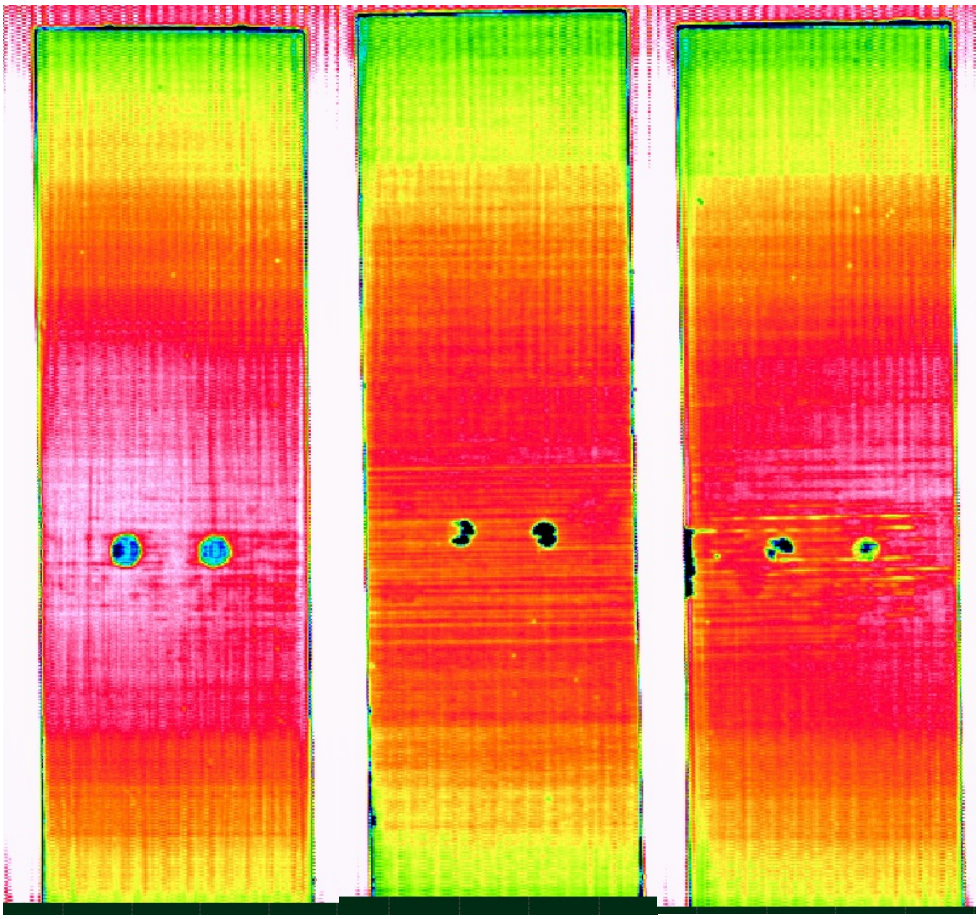

ESI 3.10 : *Ultrasonic imaging of laminate 1 (left), laminate 3 (middle), and laminate 4 (right)*

3.9 References

[1] B. Ashrafi, M.B. Jakubinek, Y. Martinez-Rubi, M. Rahmat, D. Djokic, K. Laqua, D. Park, K.-S. Kim, B. Simard, A. Yousefpour, Acta Astronautica 2017, 141, 57.

[2] R.M.A. Khan, I.E. Tabrizi, H.Q. Ali, E. Demir, M. Yildiz, Polymer Testing 2020, 90, 106653.

[3] G. Mook, J. Pohl, F. Michel, T. Benziger, A. Hilbig, in Materials for Transportation Technology, 2000, 198.

[4] R. de Oliveira, C.A. Ramos, A.T. Marques, Computers & Structures 2008, 86, 340.

[5] A. Gullapalli, V. Beedasy, J.D.S. Vincent, Z. Leong, P. Smith, N. Morley, Advanced Engineering Materials 2021, 23, 2100313.

[6] J.S. Chilles, A.F. Koutsomitopoulou, A.J. Croxford, I.P. Bond, Composites Science and Technology 2016, 134, 81.

[7] A. Huijer, C. Kassapoglou, L. Pahlavan, Sensors 2021, 21.

[8] R. Janeliukstis, D. Mironovs, Mechanics of Composite Materials 2021, 57, 131.

[9] X. Cheng, X. Cao, Z. Wu, Z. Ying, D. Camilleri, X. Hu, Advanced Engineering Materials 2023, n/a.

[10] A. Winkler, N. Modler, W.-G. Drossel, T. Mäder, C. Körner, Advanced Engineering Materials 2018, 20, 1801001.

[11] Y. Lv, L. Min, F. Niu, Z. Qin, M. Zhang, B. Zhao, Y. Liu, K. Pan, Advanced Materials Technologies 2023, 8, 2201886.

[12] A. Winkler, N. Modler, T. Weber, O. Täger, Advanced Engineering Materials 2018, 20, 1800588.

[13] T. Karagiannis, E.F. Karachalios, N.D. Alexopoulos, Material Design & Processing Communications 2021, 3, e191.

[14] Ç. Yılmaz, H.Q. Ali, M. Yıldız, Polymer Composites 2023, 44, 2956.

[15] O. Frazão, R. Oliveira, I. Dias, Microwave and Optical Technology Letters 2009, 51, 235.

[16] J.A. Etches, G.F. Fernando, Polymer Composites 2009, 30, 1265.

[17] J.A. Etches, G.F. Fernando, Polymer Composites 2010, 31, 284.

[18] J. Barragán, A. Kell, X. Liu, S. Shin, C. Mandache, D. Djokic, D. Bennett, K. Houlahan, M. Genest, B.H. Lessard, C. Paquet, Adv Eng Mater 2025, 27, 2401332.

[19] S. Geller, T. Tyczynski, M. Gude, S. Sauer, W.-J. Fischer, Advanced Engineering Materials 2018, 20, 1800447.

[20] J. Missinne, N. Teigell Benéitez, A. Lamberti, G. Chiesura, G. Luyckx, M.-A. Mattelin, W. Van Paepegem, G. Van Steenberge, Advanced Engineering Materials 2018, 20, 1701127.

[21] M. Majumder, T.K. Gangopadhyay, A.K. Chakraborty, K. Dasgupta, D.K. Bhattacharya, Sensors and Actuators A: Physical 2008, 147, 150.

[22] J. Shi, D. Kong, C. Li, R. Guo, G. Xian, H. Liu, X. Tan, Polymer Composites 2025, 46, 5419.

[23] I. Read, P. Foote, S. Murray, Meas. Sci. Technol. 2002, 13, N5.

[24] R. Toivola, S.-H. Jang, S. Baker, A. Jen, B. Flinn, Sensors 2018, 18, 1362.

[25] R.J. Ditchburn, S.K. Burke, NDT & E International : Independent Nondestructive Testing and Evaluation 2005, 38, 690.

[26] K. Koyama, H. Hoshikawa, G. Kojima, Journal of Pressure Vessel Technology 2013, 135, 041501.

[27] T. Wang, D. Wu, W. Chen, J. Yang, Composite Structures 2021, 268, 114012.

[28] NBC Meshtech Americas, 2023.

[29] A.J. Kell, C. Paquet, O. Mozenson, I. Djavani-Tabrizi, B. Deore, X. Liu, G.P. Lopinski, R. James, K. Hettak, J. Shaker, A. Momciu, J. Ferrigno, O. Ferrand, J.X. Hu, S. Lafrenière, P.R.L. Malenfant, ACS Applied Materials & Interfaces 2017, 9, 17226.

[30] Catspit Screen Print Supply, Catspit Screen Print Supply - Phoenix, Arizona 2023.

[31] K. Wagner, S. Zou, Y. Martinez-Rubi, A.J. Kell, C. Paquet, B.H. Lessard, FPE 2023, 8, 25005.

[32] X. Liu, D. Li, H. Fukutani, P. Trudeau, L. Khoun, O. Mozenson, K.L. Sampson, M. Gallerneault, C. Paquet, T. Lacelle, B. Deore, O. Ferrand, J. Ferrigno, P.R.L. Malenfant, A.J. Kell, Adv Elect Materials 2021, 7, 2100194.

.

4. Conclusions and future work

The bulk of this thesis has consisted in developing, optimizing, and testing embedded sensors for next generation composite materials. The development of these sensors presents a significant leap in capabilities from existing measurement technologies. Thanks to their small size, which falls below the defect inclusion threshold for composites, these sensors do not affect the performance of the part in which they're embedded and therefore will not result in defects such as delamination. Furthermore, the usage of screen printing as main manufacturing method allows for a very low overall cost and comparatively simple manufacturing process. Additionally, these sensors are designed to be measured with existing, and industry standard, eddy current non-destructive analysis tools, which allows for easier adoption once the technology is further developed. The sensors are very robust, allowing for survival throughout the entire manufacturing process, including the high temperature and pressure environments which are necessary to cure aerospace grade composites. In stark comparison, and as shown by the literature review, current technologies are fragile, expensive to develop, impact the performance of the composite once in place, and require precise control of the environment to provide accurate data.

Aware of existing non-destructive testing technologies limitations, the NRC Aerospace Research Centre team gave us at the very beginning of the project several stringent minimum requirements in order to consider our sensors viable, as well as some KPI's that would be interesting to track in a composite via embedded sensors; these included limitations in size (smaller than 161 mm^2), thickness (thinner than half a ply of pre-impregnated composite, 0.0675 mm), survivability (200°C to -200°C, 0 to 6 bar) and performance (readable through at least 4mm of composite, the industry standard highest thickness for a part). They also suggested that the ability to monitor ply migration, manufacturing defects, damage, strain, and temperature would be

incredibly useful in such a package. In other words, they gave us their idea of a dream sensor to monitor performance in a composite and told us what it would take to call it a success.

With that in mind, we started the development of this new technology over 2 years ago ,and today, we have solid results to show for it, as each chapter of this thesis detailed.

Chapter 2, which was published in Advanced Engineering Materials, presents a proof of concept for the first iteration of our sensors. It laid down all the groundwork for future advancements. First, the type of ink for the sensors had to be developed, optimized, and tested for best signal readout in the EC analysis equipment. At the same time, the best parameters for the EC equipment had to be found, as scanning this type of sensor had never been done before, which left us with no starting point. Once the ink and the EC settings had been vetted, the architecture of the sensor itself had to be developed and optimize to achieve the ambitious signal return performance expected out of the sensors. Four different architectures were developed and tested, out of which double-side-printed, copper plated sensors performed the best, and were able to meet all the size, thickness, survivability and performance requirements for the minimum viable prototype. Once embedded, they were used to measure the ply migration of the different layers of a composite material throughout the different stages of manufacturing. It was found that the sensors were able to report on ply migration with an accuracy of 0.6mm in composites over 3mm thick. Lastly, x-ray and CT imaging were conducted to validate that the sensors did not result in delamination of the composite, therefore confirming that they did not affect composite material performance at that size. However, we were not able to test for changes in signal in the composite matrix after damage, this would be the main goal of our second paper.

Chapter 3 proposes a new generation of sensors that can perform the functions of the first iteration whilst still respecting the stringent requirements, but will also have the ability to measure

strain and damage to the composite. To do this, new sensor shapes were developed. In addition to the coils of the first paper, which were kept to be used as a baseline, we introduced concentric rings, and discs. These new shapes allowed for a reduction in manufacturing complexity, since the previously presented coil sensors required manual connection of both terminals of the coil, in addition to copper plating in order to obtain the desired signal return performance. The discs and rings on the other hand, had no need for additional intervention once manufactured, or for copper plating to increase the signal output. Instead, in order to increase the signal, multiple layers were printed on the sensor. This resulted in a minimal increase in thickness, which was still far from reaching the maximum allowed thickness for the sensors, but increased the signal considerably. IT was found that a disc sensor performed as well as the double-sided copper plated sensor in the first paper, and that a triple layered disc had a performance three times better than them. Once the architecture had been defined, embedding trials were made to validate their performance in strain and damage sensing. Several key lessons were learnt, that will shape future work in this technology. Firstly, it was found that only sensors directly in contact with the composite (as opposed to fully encapsulated in polyimide film, as had been done previously) showed a significant change in signal under stress, and a permanent change in signal after matrix damage. Furthermore, it was found that the substrate on which the sensor is printed plays a kay role in its performance, that is to say, the sensors that were printed on 1 mil polyimide showed a change in signal during strain, and a permanent lose after damage. On the other hand, those printed on 5 mil polyimide showed a change in signal only when under strain, and no loss after matrix damage. To help us validate the fact that it was composite matrix damage being measured, and not the sensor itself being damaged, control sensors were embedded that were fully encapsulated in polyimide. It was shown that even after complete matrix failure, the fully encapsulated sensors showed no permanent

loss in signal, and only minimal signal change when under strain. Ultrasonic and x-ray imaging was taken in order to validate the damage suffered by the composite.

Future work will focus developing technologies and printing methods that will allow the sensor print to be completely detached from the substrate. The specific method and protocol haven't been published yet but consist of screen printing and additional top and bottom dielectric layers which can be easily peeled from the polyimide substrate. This will allow to remove the influence of the polyimide substrate, which was shown to have a dampening effect on the strain and damaging measurement capabilities of the sensors. Additionally, new equipment has been made available at the Quantum and Nanotechnologies centre will allow for much more consistent double and triple layered prints, reducing the variation in the performance of the sensors. Once the new substrate-less sensors have been properly validated, further optimization on sensor size and manufacturing can be done, to reduce it even further in size as well as allow for larger scale manufacturing and implementation on several projects. It would also be interesting to characterize the strain performance of the sensor with people that have a more mechanical background, as it would allow for comparison with existing stress and strain gauging technology. As an ultimate goal, it would be interesting to further develop the technology into temperature sensing, which had been a part of the project in the past but deemed out of reach due to limitations in development back when the project started.